Max-Planck-Institut für Meteorologie
Max Planck Institute for Meteorology

Report No. 350

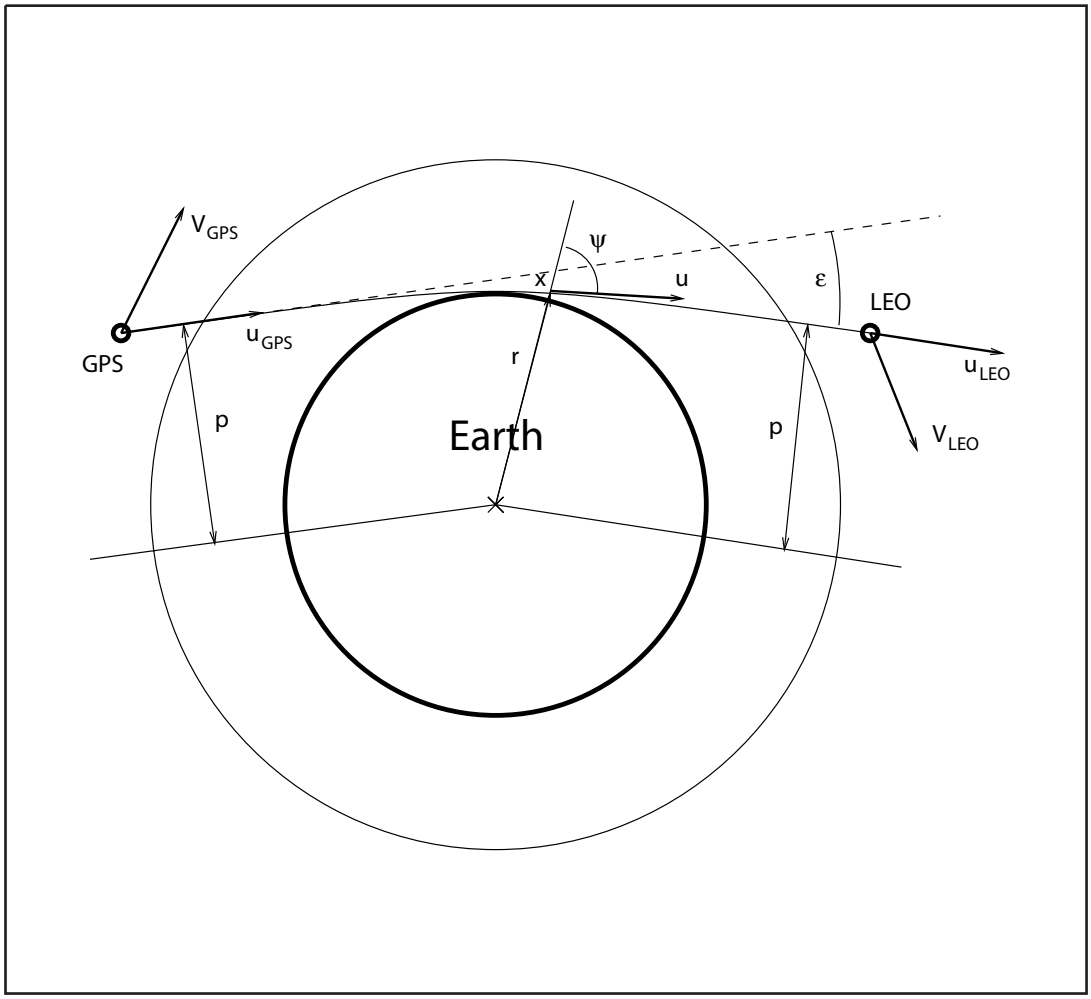

Principles of variational assimilation of GNSS radio occultation data

by

Michael E. Gorbunov • Luis Kornblueh

Hamburg, December 2003

Authors

Michael E. Gorbunov — Institute for Atmospheric Physics, Russian Academy of Sciences, Moscow, Russia

Luis Kornblueh — Max Planck Institute for Meteorology, Hamburg, Germany

Max-Planck-Institut für Meteorologie
Bundesstrasse 55
D - 20146 Hamburg
Germany

Tel.: +49-(0)40-4 11 73-0
Fax: +49-(0)40-4 11 73-298
e-mail: <name>@dkrz.de
Web: www.mpimet.mpg.de

Michael E. Gorbunov[1] and L. Kornblueh

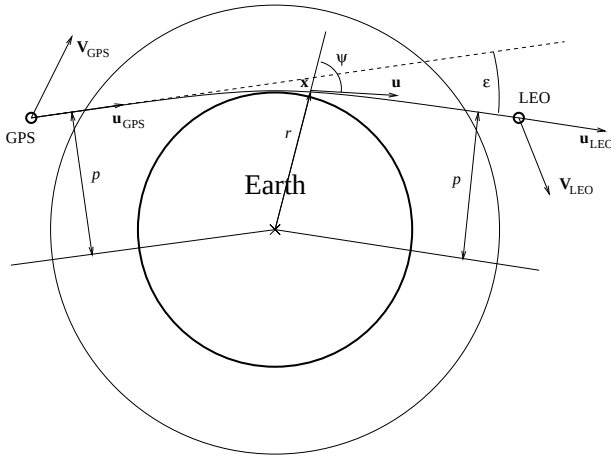

Principles of variational assimilation of GNSS radio occultation data

December 2003

[1]Institute for Atmospheric Physics, Russian Academy of Sciences, Moscow, Russia

Contents

Abstract

The standard processing of the Global Navigation Satellite System (GNSS) based refractometric data performed by means of a space-borne GPS-receiver was based on the approximate derivation of the local vertical profiles of the atmospheric refractivity by means of the Abel transform. Being sufficient at the stage of a proof-of-concept experiment, this approach results in significant errors of the reconstruction of the tropospheric refractivity both due to its complicated spatial structure at heights below 10 km and due to the impossibility of separation of the effects of dry air and water vapor without use of additional information. As has been recognized, the most promising way of utilizing GNSS radio occultation data is their variational assimilation (3D/4DVar) into a Numerical Weather Prediction Model. Nevertheless practical implementation of variational assimilation of the radio occultation data has proved to be impossible without a careful theoretical investigation of the problem. The main difficulty arises due to the atmospheric refraction representing a complicated nonlinear integral functional of the global atmospheric fields. In this report, we describe the principles of the variational assimilation of GNSS data. The investigation of the problem is based on a model of radio occultation experiments that includes the physical model of the measurements, the model of the atmospheric refractivity, and the model of wave propagation in the atmosphere. The latter was designed in two variants: i) a model based on the scalar diffraction theory which allows for accurate simulation of the diffraction and multipath effects especially important in the lower troposphere; ii) a geometric optical model that allows for fast computations. Using the standard approach, we elaborate the linear tangent and linear adjoint model for the GNSS observations, creating thus all the necessary instrumentary for the implementation of variational data assimilation systems. This is complemented with a program for primary processing of the real measurements and preparation of the input data for their assimilation into a Numerical Weather Prediction Model. The algorithms are completed in the form of a working program code.

1 Introduction

1.1 GPS/MET measurements, their processing and utilization

The radio occultation measurements have been playing a very important role in the exploration of the atmospheres of the planets in the solar system (Kliore et al., 1965; Fjeldbo and Eshleman, 1968; Lindal et al., 1990; Lindal, 1992). This measurements have always been stimulating theoretical investigations of the possibility of the application of this technique to the Earth's atmosphere as well (Phinney and Anderson, 1968; Tatarskii, 1968; Lusignan et al., 1969; Sokolovskiy, 1990; Gorbunov, 1990). But, unlike the atmospheres of the other planets, where almost any new information is of importance, for the Earth's atmosphere, the abundance of data and new applications, such as the numerical weather prediction, raised significantly the accuracy requirements. The first radio occultation soundings of the Earth's atmosphere (Rangaswamy, 1976; Yakovlev et al., 1995) were not yet able to satisfy these requirements.

The situation changed significantly with the advent of the GPS system. The use of the GPS system for the radio occultation measurements was suggested by Gurvich and Krasil'nikova (In Russian 1987, In English 1990) and Melbourne et al. (1988). The GPS system containing 24 operational satellites implemented with high-precision radio transmitters is capable of providing both a high accuracy of the measurements of the atmospheric refraction, and a good coverage of the Earth's surface. This makes the GPS measurements able to concurrent with other data sources for the operational meteorology. Further advantages of the radio occultation technique are its weather independence and its capability of performing observations over the oceans, which is especially valuable for the numerical weather prediction, whose quality suffered due to the lack of data above such a big area.

The results of the first proof-of-concept experiment with the satellite Microlab-1 implemented with a GPS-receiver (launched on April 3, 1995) indicated big capabilities of the radio occultation method in its application to the investigation of the Earth's atmosphere (Ware et al., 1996). This experiment also gave an insight into the difficulties arising in processing and utilization of the radio refractometric data.

The basic method of processing of the radio refractometric data till recently has been the Abel inversion (Phinney and Anderson, 1968; Fjeldbo and Eshleman, 1968) in the approximation of the local spherical symmetry, i.e. neglecting the horizontal gradients of the atmospheric refractivity in the vicinity of the ray perigees (Ware et al., 1996; Kursinski et al., 1996; Gorbunov et al., 1996b; Hocke, 1997; Anthes et al., 1997; Kuo et al., 1997; Rocken et al., 1997). Although just the horizontal structure of the atmospheric parameters, such as the temperature or relative humidity, represents the weather variations, and is thus of the main interest, the accuracy of this approximation was sufficient at the stage of a proof-of-concept experiment. Theoretical investigations of the potential accuracy and horizontal resolution of the Abelian inversion (Gorbunov and Sokolovskiy, 1993; Gorbunov et al., 1996a) indicated that its errors become significant in the lower troposphere due to the complicated structure of the humidity field.

Numerical simulations of the tomographic reconstruction of the global atmospheric fields from the refractometric measurements performed by a multi-LEO satellite system (Gorbunov and Sokolovskiy, 1993; Gorbunov et al., 1996a) indicated that the number of the LEO satellites necessary for accurate reconstruction of the horizontal structure in the lower troposphere at a resolution of a Global Atmospheric Circulation Model is estimated at hundreds. Such a big amount of LEO satellites is, however, extremely unlikely to become available in the near future.

As became clear, the the most promising way of utilizing refractometric data is their variational assimilation (3D/4DVar) into a Global Atmospheric Circulation Model (Eyre, 1994; Zou et al., 1995). This approach has very strong advantages as compared to the tomographic reconstruction of the global atmospheric fields. It is capable of assimilating any amount of data without resulting in high-frequency artifacts due to insufficient resolution, usual in the standard tomography. This advantage makes the variational approach especially valuable in the situation when only one LEO satellite is available, and it is impossible to arrange a tomographic high-resolution scanning of the atmosphere. This method is also capable of assimilating any kind of measured data in an unique way. The problem of separation of the humidity and temperature influence on the refractivity (Gorbunov and Sokolovskiy, 1993; Gorbunov et al., 1996a) is also solved in this method automatically (Zou et al., 1995).

But practical implementation of 3d/4DVar of the GPS/MET data was compelled to wait for a series of theoretical problems to be resolved. The main problem consisted in the fact that the refractometric measurements represent some complicated nonlinear integral functionals of the global atmospheric fields. Thus assimilation of each data must result in correction of the atmospheric state along all the ray rather than near its perigee only.

Being based on solving for the most probable atmospheric state defined both by the model dynamical equations and by the error bars of the observations, 3D/4DVar requires the Global Atmospheric Circulation Model to be complemented with the observation operator. This operator transforms the gridded fields of the model variables representing an atmospheric state, into the observables, and the derivatives of the observation operator with respect to the model variables. For the refractometric measurements, the construction of the observation operator is rather straightforward and based on the ray-tracing algorithms (Gorbunov et al., 1996a,b; Syndergaard and Høeg, 1996), but its differentiation with respect to the model variables is a much more complicated problem.

This problem was solved by differentiating the geometric optical observational operator on the code level (Zou et al., 2000). Assimilation of GPS/MET using this technique was described in (Liu et al., 2001), and it was found that the impact of GPS/MET observation is small. Further improvements of this scheme were described in (Liu and Zou, 2003). In those works, very large mismatches between observed and simulated impact parameters were revealed. The mismatches can reach 600 m. This suggests that there are some mistakes in the parameterization of the oculltation geometry, which must impair the quality of results. Another sourse of errors is the definition of the refraction angle as the angle between ray directions at the transmitter and receiver.

In this report, we describe a refractometric algorithm usable for 3D/4DVar assimilation of GPS/MET data. The algorithms include: i) a module of the primary processing of the GPS/MET radio occultation data for the derivation of the atmospheric refraction; ii) the observation operator deriving the model refraction from the gridded fields of the model variables; iii) the linear tangent model of the atmospheric refraction that allows for the calculation of the first-order perturbations of the observables from variations of the model variables; iv) the linear adjoint model of the atmospheric refraction that allows for the calculation of the derivatives of the observation operator with respect to the model variables.

The differences between our algorithm and that described in (Liu et al., 2001; Liu and Zou, 2003) are the following: 1) We use the definition of the refraction angle through the Doppler frequency shift, which matches the definition of the refraction angle derived from radio occultation data. The difference between these two definition can be significant in the lower troposphere. 2) We use more accurate parameterization of the geometry, which results in accurate match of modeled and observed impact parameters. 3) We use the differentiation of the model on the analytical level.

An important, but missing part is the model of the measurement errors. As was shown in (Gorbunov et al., 1996a), the basic error of the measurements of the refraction angle in the height range 10 – 90 km is the residual error of the removal of the ionospheric effect. The statistical characteristics of this noise can be derived from refraction angle profiles at heights above 60 km, where it constitutes the dominant part of measurements. At heights below 30 km, its influence on the reconstruction of the atmospheric refractivity is, however, very weak. Investigation of the refraction angle profiles by means of the methods of the diffraction theory (Gorbunov et al., 1996b) indicates that in the lower troposphere (below 10 km), the refraction angle profiles undergo very strong scintillations due to the complicated structure of the atmospheric humidity, which is the signature of the atmospheric turbulence. The turbulent structure is not reproduced by Global Atmospheric Circulation Models and must be looked at as a source of the measurement noise which will be dominant in the lower troposphere. Creation of a model of this noise is an important problem for a future investigation.

2 Observation operator, linear tangent and linear adjoint models for the refractometric measurements

2.1 Variational assimilation of the refractometric measurements

The general principle of the variational data assimilation consists in solving for the most probable atmospheric state defined both by the measurements and dynamical equations. The *a posteriori* probability density of the atmospheric state $\mathbf{X}$ can be represented as the normed product of its *a priori* probability density computed on the basis of its background estimation (forecast) $\mathbf{X_b}$ and the probability density of the vector of the observables $\mathbf{Y}$:

$$P(\mathbf{X}|\mathbf{Y}) = \frac{1}{N} P(\mathbf{X}|\mathbf{X_b}) P(\mathbf{Y}|\mathbf{X}) \tag{2.1.1}$$

where N is the norming constant.

Assuming that both background estimation errors and measurement errors have the Gaussian statistics and are independent on each other, we can write the explicit expression of the probability density:

$$P(\mathbf{X}|\mathbf{Y}) = \frac{1}{N}\exp\left(-\frac{1}{2}(\mathbf{Y}-H(\mathbf{X})(O+F)^{-1}(\mathbf{Y}-H(\mathbf{X})^T - \frac{1}{2}(\mathbf{X}-\mathbf{X_b})B^{-1}(\mathbf{X}-\mathbf{X_b})^T\right) \tag{2.1.2}$$

where $\mathbf{Y}$ is the vector of the real measurements, H is the observation operator, O is the covariance matrix of the measurement errors, F is the covariance matrix of the errors in the observation operator, B is the covariance matrix of the background estimation errors. This results in the necessity of minimization of the following quadratic form (Eyre, 1994):

$$J(\mathbf{X}) = \frac{1}{2}(\mathbf{Y}-H(\mathbf{X}))(O+F)^{-1}(\mathbf{Y}-H(\mathbf{X}))^T + \frac{1}{2}(\mathbf{X}-\mathbf{X_b})B^{-1}(\mathbf{X}-\mathbf{X_b})^T \tag{2.1.3}$$

which requires knowledge of its gradient:

$$\nabla_{\mathbf{X}} J(\mathbf{X}) = -H'(\mathbf{X})(O+F)^{-1}(\mathbf{Y}-H(\mathbf{X})^T + B^{-1}(\mathbf{X}-\mathbf{X_b})^T \tag{2.1.4}$$

where $H'(\mathbf{X})$ is the Fréchet derivative of the observation operator.

Equations (2.1.3, 2.1.4) are the basis for variational data assimilation.

Assuming now that we have a series of measurements $\mathbf{Y}$ at moments of time $t_0..t_R$ and background estimation $\mathbf{X_b}$ is a function of time and initial condition $\mathbf{X_0}$ at moment t_0, we can find the most probable initial condition, whose conditional probability density can be written as follows:

$$P(\mathbf{X_0}|\mathbf{Y}(t_0),...,\mathbf{Y}(t_N)) = \frac{1}{N}\prod_{r=0}^{R} P\left(\mathbf{Y}(t_r)|\mathbf{X_b}(t_r,\mathbf{X_0})\right) \tag{2.1.5}$$

Assuming again the Gaussian statistics of the errors, we arrive at the necessity of the minimization of the following form (which is similar to that used in (Zou et al., 1995)):

$$J(\mathbf{X_0}) = \sum_{r=0}^{R}\left(H(\mathbf{X_b}(t_r,\mathbf{X_0})) - \mathbf{Y}(t_r)\right)(O+F)^{-1}\left(H(\mathbf{X_b}(t_r,\mathbf{X_0})) - \mathbf{Y}(t_r)\right)^T \tag{2.1.6}$$

which requires knowledge of its gradient

$$\nabla_{\mathbf{X_0}} J(\mathbf{X_0}) = \sum_{r=0}^{R} H'(\mathbf{X_b}(t_r,\mathbf{X_0}))\frac{\partial \mathbf{X_b}(t_r,\mathbf{X_0})}{\partial \mathbf{X_0}}(O+F)^{-1}\left(H(\mathbf{X_b}(t_r,\mathbf{X_0})) - \mathbf{Y}(t_r)\right)^T \tag{2.1.7}$$

Equations (2.1.6, 2.1.7) are the basis of the 4D variational assimilation.

From the general view point, the principles of assimilation of the atmospheric refraction are the same as those of any other kind- of measurements. The following three model components are required as are: i) the observation operator; ii) its linearization (tangent linear); iii) the linear adjoint model that allows the derivatives of the observation operator with respect to the model variables to be calculated.

The observation operator corresponding to the refractometric measurements must describe the propagation of radio waves in the atmosphere and derive the values observed in radio occultation experiments. The basic approximation at this step is the geometrical optics. Although the accuracy of the geometrical optics is satisfactory for the wave length and geometry of the GPS/MET measurements, sometimes it is useful to have a complete model based on the diffraction theory. Such a model is especially important for the generation of artificial data for the investigation of the capabilities of a GPS-receiver.

Given the satellite positions and velocities, we can find a geometric optical ray between them for a given state of the atmosphere and the corresponding Doppler frequency shift. For a spherically layered atmosphere, complementing the Doppler frequency shift with Snell's law we can find refraction angle ϵ and ray impact parameter p (Vorob'ev and Krasil'nikova, 1994; Gorbunov et al., 1996a).

Although the real atmosphere is not spherically layered, we will calculate $\epsilon(p)$ using the assumption of the spherical symmetry. That does not imply any contradiction with the fact that the purpose of 4DVar is just to eliminate this assumption used in the standard inversion technique. In order to see that, we can accept the view at $\epsilon(p)$ as a known functional of the model variables and the observation geometry, that can be reproduced in the observation operator.

Another possibility could be assimilation of the Doppler frequency shift as the function of the satellite positions (corrected for the ionospheric refraction angle (Gorbunov et al., 1996a)). This would allow some approximations connected with the observation geometry to be avoided and would even be preferable, but not for the multipath propagation which makes this dependence non-unique in the lower troposphere.

Derivation of both linear tangent and linear adjoint models can be based on the general principles (Hoffman et al., 1992). For a given ray, we can now introduce 6D state vector $\mathbf{z}(\tau)$ compounded of two 3D vectors $\mathbf{x}(\tau)$ and $\mathbf{u}(\tau) = \dot{\mathbf{x}}(\tau)$ representing the ray trajectory and its direction, τ being the trajectory parameter. Our observation operator is based on the numerical integration of the ray trajectory equation. Given a discrete integration scheme (say the Runge - Kutta method), the trajectory can be represented as a discrete set of points $\mathbf{z}_n$, $n = 0..N$, the transfer to $\mathbf{z}_{n-1}$ to $\mathbf{z}_n$ being performed by a non-linear operator F_n that depends on the refractivity gradients α^{μ}_{n-1} at some points $\mathbf{x}^{\mu}_{n-1}$ involved into the calculation of $\mathbf{z}_n$ (for the Runge - Kutta scheme of the fifth order, $\mu = 1..4$). Thus our model can be assumed to have a set of parameters $\alpha^{\mu}_n = \mathbf{a}_n$.

The linear tangent model can then be written as follows:

$$\delta\mathbf{z}_n = \hat{\mathbf{B}}_n \delta\mathbf{z}_{n-1} + \hat{\mathbf{C}}_n \delta\mathbf{a}_{n-1} \tag{2.1.8}$$

where $\hat{\mathbf{B}}_n$ and $\hat{\mathbf{C}}_n$ are corresponding Fréchet operator derivatives (from the computational point of view, simply matrices). The linear adjoint model can now be derived in the standard way. The refraction angle and impact parameter depend on $\mathbf{z}_0$ and $\mathbf{z}_N$, and using the linear tangent and linear adjoint models, we can calculate the variations and derivatives of function $\epsilon(p)$ with respect to parameters $\mathbf{a}_n$.

All the previous consideration did not depend on which Global Atmospheric Circulation Model we use. This dependence appears at the next step, when we have to calculate the variations and derivatives of the refractivity gradients α_n^μ at points $\mathbf{x}_{n-1}^\mu$ with respect to the atmospheric state parameters such as temperature T_{ijk}, humidity q_{ijk} and surface pressure $P_{s,jk}$. This calculation can be performed on the basis of the relationship between the atmospheric parameters and refractivity, and the interpolation scheme of the atmospheric refractivity for its usage in the ray tracing (Gorbunov et al., 1996a,b). It must be also taken into account, that the geometrical heights of the model grid points depend on the model variables (DKRZ, 1994). This done, the derivative of the refraction angle with respect to the model parameters can be expressed as follows:

$$\frac{\partial \epsilon(p)}{\partial (T_{ijk}, q_{ijk}, P_{s,jk})} = \frac{\partial \epsilon(p)}{\partial \mathbf{a}_n} \frac{\partial \mathbf{a}_n}{\partial (T_{ijk}, q_{ijk}, P_{s,jk})} \tag{2.1.9}$$

(Here and further we follow the standard rule of the calculus of tensors implying Einsteins summation convention). Such a subdivision allows for the maximum flexibility of the algorithms and simplifies their modification for different atmospheric models.

The first example of a numerical computation of the derivatives of the refraction angle with respect to the model variables was given by (Eyre, 1994). The calculation was only designed as a demonstration and was based on the finite difference method, which cannot be used in operational applications due to its extremely high requirements of computational time.

2.2 The physical model of radio occultation experiments

The physical model of radio occultation experiments is based on the concept of electromagnetic waves propagating in an inhomogeneous medium. The wave lengths used in the GPS/MET measurement (19 and 24 cm) are very small as compared to the characteristic scale of atmospheric inhomogeneities, and thus the effects of back scattering and depolarization are negligible, which allows for the usage of the scalar diffraction theory (Tatarskii, 1961). The scalar Helmholtz equation with the harmonic time dependence removed can be written as follows:

$$\Delta U(\mathbf{x}) + k^2 n^2(\mathbf{x}) U(\mathbf{x}) = 0 \tag{2.2.1}$$

where U is the complex amplitude of electromagnetic field depending on the spatial coordinate vector $\mathbf{x}$, n is the refractive index of the medium, $k = \dfrac{2\pi}{\lambda}$ is the free-space wave number, λ is the wave length.

Calculation of the electromagnetic field in the atmosphere can be performed using the split-step method (Martin, 1992). Although being time-consuming, which at present makes impossible its usage in operational applications, such a model is necessary as a reference point for further approximations.

A fast computational model of refractometric experiments can be based on the geometrical optics, or WKB approximation (Kravtsov and Orlov, 1990; Weng Cho Chew, 1994). For its derivation, we use representation $U = A\exp(ik\Phi)$ of complex field U through its amplitude A and phase Φ which we assume to change very slowly within the scale of the wave length. Substituting it into (2.2.1) and collecting the most significant terms proportional to k^2, we arrive at the eikonal equation (Kravtsov and Orlov, 1990):

$$(\nabla\Phi)^2 = n^2 \tag{2.2.2}$$

This is a differential equation of the 1st order, whose characteristic equation has the following form:

$$\frac{dx_i}{2u_i} = \frac{du_i}{2n\partial n/dx_i} = \frac{d\Phi}{2\mathbf{u}^2} = \frac{d\tau}{2} \tag{2.2.3}$$

where $\mathbf{u} = \nabla\Phi$, and thus $\mathbf{u}^2 = n^2$. This results in the equation of geometric optical rays:

$$\begin{aligned} \frac{d\mathbf{x}}{d\tau} &= \mathbf{u} \\ \frac{d\mathbf{u}}{d\tau} &= n\nabla n \end{aligned} \tag{2.2.4}$$

The relation between trajectory parameter τ and ray arc length s can be derived from the first equation: $d\tau^2 = d\mathbf{x}^2/\mathbf{u}^2 = ds^2/n^2$, and thus $d\tau = ds/n$.

The geometrical optics provides a very convenient basis for the description of radio occultation experiments. Thus we are able to introduce the refraction (bending) angle and ray impact parameter (Figure 1). Refraction angle ϵ is defined as the angle between ray direction before and after passing the atmosphere. Ray impact parameter p is very convenient for the description of refraction in spherically layered media, and it is defined as the distance between the symmetry center and the straight line continuation of the ray in vacuum (ray leveling distance from the Earth's center). More generally, it can be defined as the ray invariant:

$$p = rn(r)\sin\psi \tag{2.2.5}$$

where r is the distance from the symmetry center, and ψ is the angle between the ray direction and the radius vector of the current point of the ray. This equation is known as Snell's law for spherically layered media (Kravtsov and Orlov, 1990). Dependence $\epsilon(p)$ can be transformed to $n(r)$ by means of the Abel transform (Phinney and Anderson, 1968).

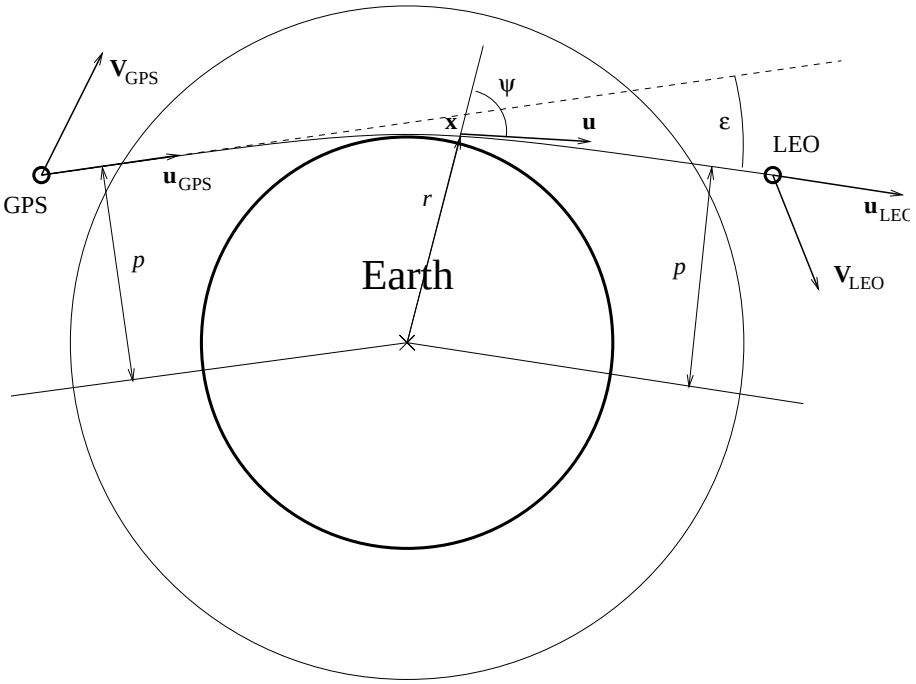

Figure 1: The geometry of radio occultations.

Although the real atmosphere is not spherically symmetrical, and Snell's law is broken, the same inversion technique can be applied also in this case, providing an approximate solution of the inverse problem (Ware et al., 1996; Kursinski et al., 1996; Gorbunov et al., 1996a,b; Hocke, 1997).

The criterion of the applicability of the geometrical optics is based on the concept of the Fresnel zone that is defined as the area exerting the most significant influence on the forming of the wave field at a given observation point. For a given ray, the Fresnel zone size in the transversal direction is estimated as $\sqrt{L\lambda}$, where L is the distance to the observation point. Thus a geometric optical ray may be thought to be surrounded by a volume representing a physical ray. The geometrical optics can only be applied when the characteristic scale of the atmospheric inhomogeneities in the direction transversal to the ray is smaller than or comparable with the Fresnel zone size. Although constituting the natural limit of the spatial resolution when solving the inverse problem in the geometric optical approximation, the Fresnel zone size is by no means its principal limit.

For the GPS/MET observations, the distance between the observer and the ray perigee point is about 3000 km, which results in a Fresnel zone size of about 1 km, but in the lower troposphere, due to the strong regular refraction, its vertical dimension dwindles by a factor of $\left(1 - L\frac{d\epsilon}{dp}\right)^{1/2}$ (Melbourne et al., 1994), which reaches a value of about 10 on the Earth's surface. This estimation indicates that the vertical discretization step of an atmospheric model with 19 vertical levels does not exceed the Fresnel zone size, and the observation operator of the refractometric measurements can be based on the geometrical optics.

In a radio occultation experiment, direct measurements of the refraction angle are conjugated

with big technical difficulties. Instead, the Doppler frequency shift is measured, and using its relation to the ray geometry, one can calculate the refraction angle and impact parameter.

The derivation of the expression for the Doppler shift is based on the fact that angular frequency ω and wave vector $\mathbf{k}$ of an electromagnetic wave are the time and space components of a 4-vector with its 4-length $\omega^2 - c^2\mathbf{k}^2 = 0$, c being the light velocity in vacuum. When transferring to another coordinate frame moving with velocity $\mathbf{V}$ with respect to the reference one, the 4-vector is subject to the Lorenz transform, and thus we derive the transformation law for the frequency:

$$\omega' = \frac{\omega - \mathbf{V}\mathbf{k}}{\sqrt{1 - \dfrac{V^2}{c^2}}} = \omega \frac{c - \mathbf{V}\mathbf{u}}{\sqrt{c^2 - V^2}} \tag{2.2.6}$$

where ω and $\mathbf{k}$ are the frequency and wave vector in the reference frame, respectively, $\mathbf{u} = \mathbf{k}/k = c\mathbf{k}/\omega$ is the wave direction vector in the reference frame, ω' is the frequency in the moving frame.

In a radio occultation experiment, the radio signal is emitted by a GPS satellite moving with velocity $\mathbf{V}_{\mathrm{GPS}}$ and received by a LEO, whose velocity is $\mathbf{V}_{\mathrm{LEO}}$, where the velocities are given in the Earth reference coordinate frame. Introducing ray directions $\mathbf{u}_{\mathrm{GPS}}$ and $\mathbf{u}_{\mathrm{LEO}}$ at GPS and LEO in the reference coordinate frame, we can then write the relationship between emitted and received frequencies ω_{GPS} and ω_{LEO} in the moving GPS and LEO coordinate frames:

$$\omega = \omega_{\mathrm{GPS}} \frac{\sqrt{c^2 - V_{\mathrm{GPS}}^2}}{c - \mathbf{V}_{\mathrm{GPS}}\mathbf{u}_{\mathrm{GPS}}} = \omega_{\mathrm{LEO}} \frac{\sqrt{c^2 - V_{\mathrm{LEO}}^2}}{c - \mathbf{V}_{\mathrm{LEO}}\mathbf{u}_{\mathrm{LEO}}} \tag{2.2.7}$$

And thus

$$\omega_{\mathrm{LEO}} = \omega_{\mathrm{GPS}} \frac{c - \mathbf{V}_{\mathrm{LEO}}\mathbf{u}_{\mathrm{LEO}}}{c - \mathbf{V}_{\mathrm{GPS}}\mathbf{u}_{\mathrm{GPS}}} \sqrt{\frac{c^2 - V_{\mathrm{GPS}}^2}{c^2 - V_{\mathrm{LEO}}^2}} \tag{2.2.8}$$

The frequency of the signal is transformed to the optical path excess. Introducing straight line GPS-LEO direction $\mathbf{u}^{(0)}$ and corresponding "atmospheric-free" Doppler frequency $\omega_{\mathrm{LEO}}^{(0)}$:

$$\omega_{\mathrm{LEO}}^{(0)} = \omega_{\mathrm{GPS}} \frac{c - \mathbf{V}_{\mathrm{LEO}}\mathbf{u}^{(0)}}{c - \mathbf{V}_{\mathrm{GPS}}\mathbf{u}^{(0)}} \sqrt{\frac{c^2 - V_{\mathrm{GPS}}^2}{c^2 - V_{\mathrm{LEO}}^2}} \tag{2.2.9}$$

we can express the optical path excess Δs as the difference between the accumulated phase that would be observed in vacuum with the same observation geometry, and the observed one:

$$\Delta s(t) = \frac{\lambda}{2\pi} \int_{t_0}^{t} \left(\omega_{\mathrm{LEO}}^{(0)}(t') - \omega_{\mathrm{LEO}}(t') \right) dt' \tag{2.2.10}$$

The optical path excess characterizes the summary effect of the neutral atmosphere and the ionosphere. Using the relative Doppler frequency shift that can be calculated from the optical path excess data as follows:

$$d = \frac{\omega_{\mathrm{LEO}} - \omega_{\mathrm{GPS}}}{\omega_{\mathrm{GPS}}} = \frac{\omega_{\mathrm{LEO}}^{(0)} - \dfrac{2\pi}{\lambda}\dfrac{d\Delta s}{dt}}{\omega_{\mathrm{GPS}}} - 1 \tag{2.2.11}$$

and complementing it with Snell's law in the vector form, we can write the equations determining ray directions $\mathbf{u}_{\mathrm{GPS}}$ and $\mathbf{u}_{\mathrm{LEO}}$:

$$\begin{gathered} \frac{c - \mathbf{V}_{\mathrm{LEO}}\mathbf{u}_{\mathrm{LEO}}}{c - \mathbf{V}_{\mathrm{GPS}}\mathbf{u}_{\mathrm{GPS}}}\sqrt{\frac{c^2 - V_{\mathrm{GPS}}^2}{c^2 - V_{\mathrm{LEO}}^2}} - 1 = d \\ [\mathbf{x}_{\mathrm{GPS}}, \mathbf{u}_{\mathrm{GPS}}] = [\mathbf{x}_{\mathrm{LEO}}, \mathbf{u}_{\mathrm{LEO}}] \end{gathered} \tag{2.2.12}$$

This system solved, the refraction angle can be calculated as angle ϵ between $\mathbf{u}_{\mathrm{GPS}}$ and $\mathbf{u}_{\mathrm{LEO}}$, impact parameter p equals $\left|\,[\mathbf{x}_{\mathrm{GPS}}, \mathbf{u}_{\mathrm{GPS}}]\,\right|$. Interpretation of the measurements in a multipath zone, where several rays interfere at the receiver, is more complicated and requires application of the diffraction theory, as will be described below.

2.3 Model of the 3D refractivity field and its derivatives

In order to design a computational model of radio occultation experiments, a continuous model of 3D refractivity field and its derivatives is required. Particularly, the solution of the diffractive problem needs the field $n(\mathbf{x})$, the numerical integration of the geometric optical ray equation needs both $n(\mathbf{x})$ and its gradient $\nabla n(\mathbf{x})$, and the linear tangent model based on the perturbation theory requires in addition the Hessian matrix $\nabla \otimes \nabla n(\mathbf{x})$. This can be done on the basis of interpolation of a gridded field of the refractivity computed from gridded fields of the temperature, humidity, and surface pressure.

In the ECHAM3 model (DKRZ, 1994), temperature T_{ijk}, relative humidity $q_{\nu,ijk}$, and surface pressure $P_{s,jk}$ are given for the Gaussian grid of latitudes φ_j and the homogeneous grid of longitudes λ_k, at full geopotential levels ϕ_{ijk} defined from the hydrostatic equation. For T106 resolution, the indexes have the following ranges: i=1..19 for full-level quantities and i = 0..19 for half-level quantities, j = 1..160, k = 1..320. The formulas for the calculation of the half and full geopotential levels and corresponding pressure are as follows (DKRZ, 1994):

$$
\begin{gathered}
P_{i+1/2,jk} = A_{i+1/2} + B_{i+1/2} P_{s,jk} \\
P_{ijk} = \frac{1}{2}\left(P_{i+1/2,jk} + P_{i-1/2,jk}\right) \\
\phi_{i+1/2,jk} - \phi_{i-1/2,jk} = -R_d T_{\nu,ijk} \ln\left(\frac{P_{i+1/2,jk}}{P_{i-1/2,jk}}\right) \\
T_{\nu,ijk} = T_{ijk}\left(1 + \left(\frac{R_\nu}{R_d} - 1\right) q_{\nu,ijk}\right) \\
\phi_{i_{\max}+1/2,jk} = \phi_{s,jk} \\
\phi_{ijk} = \phi_{i+1/2,jk} + \alpha_{ijk} R_d T_{\nu,ijk} \\
\alpha_{ijk} = \begin{cases} \ln 2, & i = 1 \\ 1 - \dfrac{P_{i-1/2,jk}}{P_{i+1/2,jk} - P_{i-1/2,jk}} \ln\left(\dfrac{P_{i+1/2,jk}}{P_{i-1/2,jk}}\right), & i > 1 \end{cases}
\end{gathered}
\tag{2.3.1}
$$

where $A_{i+1/2}$ and $B_{i+1/2}$ are the vertical coordinate parameters, R_d and R_ν are the gas constant for dry air and water vapor respectively, $T_{\nu,ijk}$ is virtual temperature, $\phi_{s,jk}$ is surface geopotential (orography).

Given the temperature, pressure, and humidity at a grid point, the refractivity is calculated as follows (Bean and Datton, 1968):

$$
\begin{aligned}
n_{ijk} &= c_1 \frac{P_{ijk}}{T_{ijk}} + c_2 \frac{P_{w,ijk}}{T_{ijk}^2} \\
P_{w,ijk} &= \frac{q_{\nu,ijk} P_{w,ijk}}{\dfrac{R_d}{R_\nu} + \left(1 - \dfrac{R_d}{R_\nu}\right) q_{\nu,ijk}}
\end{aligned}
\tag{2.3.2}
$$

where $P_{w,ijk}$ is water vapor pressure, and the constants $c_1 = 7.76{\times}10^{-5}$ K/mbar, c_2=0.37 K^2/mbar.

For the calculation of the spatial location of a grid point, we used the reference ellipsoid model with the semi-axes being equal to 6378.1363 and 6356.7516 km, and corresponding gravity field $g(z, \varphi)$ (Lambeck, 1988), where z is the height above the Earth's surface. Model latitudes were treated as geodetic latitudes on the reference ellipsoid. Calculation of geometrical heights z_{ijk} was based on the following approximate formula (NOAA, 1976; List, 1968):

$$
\begin{gathered}
z_{ijk} = \frac{r_0 \phi_{ijk}}{g(0, \varphi_j) r_0 / g_0 - \phi_{ijk}} \\
r_0 = \frac{2 \times 10^{-3} g(0, \varphi_j)}{3.085462 \times 10^{-6} + 2.27 \times 10^{-9} \cos(2\varphi_{\mathrm{GC},j}) - 2 \times 10^{-12} \cos(4\varphi_{\mathrm{GC},j})}
\end{gathered}
\tag{2.3.3}
$$

where g_0 is the standard gravity acceleration, r_0 is the effective Earth radius, $\varphi_{\mathrm{GC},j}$ is the geocentric latitude of a grid point, the geopotential units are gpkm, r_0 and z_{ijk} are measured in km.

We shall now describe the procedure of interpolation of the gridded field of refractivity $n_{ijk} = n(z_{ijk}, \varphi_j, \lambda_k)$.

First the initialization was performed, which consisted in spline interpolation of $\ln N_{ijk} = \ln(n_{ijk} - 1)$ for each vertical profile. The interpolation coefficients were then stored.

For a given point $\mathbf{x}$ in the Cartesian coordinates, its geodetic coordinates (z, φ, λ) were calculated. Then the horizontal grid mesh $(\varphi_J..\varphi_{J+1}, \lambda_K..\lambda_{K+1})$ containing point (φ, λ) was located. Vertically interpolated values $\ln N_{jk}(z)$, $\ln' N_{jk}(z)$, $\ln'' N_{jk}(z)$ for the four pairs of indexes $j = J..J+1$ and $k = K..K+1$ were calculated. The linear interpolation of these values with respect to φ, λ-coordinates was then performed to produce $\ln N(\mathbf{x})$ and its derivatives $\ln'_z N(\mathbf{x})$ and $\ln''_z N(\mathbf{x})$ in the vertical direction.

Introducing the local vertical vector $\mathbf{v}(\mathbf{x}) = (\cos\varphi\cos\lambda, \cos\varphi\sin\lambda, \sin\varphi)$ in the Cartesian coordinates, we can approximately calculate the gradient and the Hessian matrix:

$$\begin{aligned} \nabla n(\mathbf{x}) &= \mathbf{v}(\mathbf{x}) N(\mathbf{x}) \ln'_z N(\mathbf{x}) \\ \nabla \otimes \nabla n(\mathbf{x}) &= \mathbf{v}(\mathbf{x}) \otimes \mathbf{v}(\mathbf{x}) N(\mathbf{x}) \left[\ln''_z N(\mathbf{x}) + (\ln'_z N(\mathbf{x}))^2\right] \end{aligned} \tag{2.3.4}$$

The gridded refractivity thus calculated is given in the ECHAM3 height range, i.e. at heights up to about 30 km. But accurate calculation of refraction requires knowledge of the refractivity up to a height of 120 km. At heights 30 – 120 km, we used refractivity $n_{\mathrm{CIRA}}(\mathbf{x})$ calculated from the CIRA climatological model (COSPAR, 1986) basing on an interpolation scheme similar to that described above. For a smooth transfer from exponentially extrapolated refractivity n_{ECHAM3} to n_{CIRA}, we used the following formula:

$$\begin{aligned} n(z, \varphi, \lambda) = (n_{\mathrm{ECHAM3}}(z, \varphi, \lambda) - n_{\mathrm{CIRA}}(z, \varphi)) \exp\left(-\frac{(z - z_{\max}(\varphi, \lambda))^2}{\Delta z^2}\right) + \\ + n_{\mathrm{CIRA}}(z, \varphi), \quad z > z_{\max} \end{aligned} \tag{2.3.5}$$

where $z_{\max}(\varphi, \lambda)$ is the highest model level for the given latitude and longitude, Δz=5 km.

2.4 Diffractive model

As was shown above, the geometrical optics provides a reliable basis for the observation operator of the refractometric measurements. Nevertheless it is desirable to have a more complete model of wave propagation in the atmosphere. Such a model is especially important in investigations of the lower troposphere. The complicated structure of the refraction index in the lower troposphere results in multipath propagation of radio waves, i.e. interference of several rays at the receiver. The geometrical optics is incapable of providing a good description of the wave field in a multi-path zone. In this section, we describe the diffractive model of the refractometric observations. The algorithms of processing of the signal in multi-path zones in order to extract the geometric optical refraction angle from the wave field will be described later.

The diffractive model of the radio occultation experiments is based on the split-step method (Martin, 1992), which was initially designed for the solution of the parabolic equation, and which we modified for solving the Helmholtz equation.

The split-step method consists in subdividing an inhomogeneous media into a series of thin slabs transversal to the wave propagation direction and in the description of wave propagation in each slab in the thin screen approximation, i.e. squeezing each slab into a phase screen. Thus the calculation of wave propagation in each slab is split into two sub-steps: i) instant change of the phase of the incident wave at a phase screen; ii) propagation of the wave through vacuum to the next phase screen.

As was noticed above, the Fresnel zone size for the GPS/MET observations does not exceed a value of 1 km. This is comparable with the vertical scale of the atmospheric inhomogeneities, but significantly smaller than their horizontal scale. That allows us to solve the 2D diffractive problem in the vertical occultation plane, since the diffractive effects of the horizontal structure of the atmosphere are negligible. This only applies to the case, when we neglect the investigation of the diffraction on the atmospheric turbulence, which can be important, but requires the solution of the 3D problem.

Wave propagation in vacuum is described in terms of the wave angular spectra (Zverev, 1975).

Let us consider the plane of wave propagation where we introduce Cartesian coordinates x and z, axis x pointing in the propagation direction of the incident wave, the phase screens being transversal to it. Given boundary condition $U(x = x_0, z)$ at a phase screen, we can find the corresponding representation of field $U(x, z)$ in free space as a superposition of harmonic waves $\exp(ik_x(x - x_0) + ik_z z)$. Due to the Helmholtz equation in vacuum, for each harmonic $k_x^2 + k_z^2 = k^2$, and thus $U(x, z)$ can be represented through its 1D angular spectrum $\tilde{U}(k_z)$:

$$U(x,z) = \int \tilde{U}(k_z) \exp\left(i\sqrt{k^2 - k_z^2}(x - x_0) + ik_z z\right) dk_z \tag{2.4.1}$$

Using the boundary condition, we have the following equation:

$$\int \tilde{U}(k_z) \exp(ik_z z) dk_z = U(x_0, z) \tag{2.4.2}$$

which tells us that angular spectrum $\tilde{U}(k_z)$ is simply the Fourier image of boundary condition $U(x_0, z)$. Assuming that the distance between the phase screens is δx, and thus the equivalent optical thickness of each screen is $\int_x^{x+\delta x} (n(x,z) - 1)\, dx$, we can write each step transforming $U(x, z)$ to $U(x + \delta x, z)$ as the composition of the action of the phase screen and wave propagation in vacuum described in terms of the angular spectrum:

$$\begin{gathered}
\tilde{U}(x, k_z) = \hat{F}_z \left[\exp\left(ik \int_x^{x+\delta x} (n(x,z) - 1)\, dx \right) U(x,z) \right] \\
\tilde{U}(x + \delta x, k_z) = \exp\left(i\sqrt{k^2 - k_z^2}\delta x\right) \tilde{U}(x, k_z) \\
U(x + \delta x, z) = \hat{F}_z^{-1} \left[\tilde{U}(x + \delta x, k_z) \right]
\end{gathered} \tag{2.4.3}$$

where $\hat{F}_z$ is the Fourier transform with respect to z-coordinate. The split-step algorithm can thus be implemented on the basis of FFT.

A principle limitation of the split-step method consists in its incapability of taking into account the backscattering, but it is not of any importance for GPS/MET measurements where the wave length is very small as compared to the characteristic scale of the atmospheric inhomogeneities.

Another restriction of the method consists in the fact that all the phase screens must be parallel (otherwise FFT cannot be used). This does not allow the phase screens to be turned or bent in order to compensate for the bending of the wave fronts due to the strong regular refraction in the lower troposphere. Thus a very small discretization step in phase screen planes may be required. The step can be estimated as $\lambda/(4\epsilon)$. For a characteristic tropospheric refraction angle of 0.02 and the GPS/MET wave length 20 cm, we have an estimation of the discretization step of 2.5 m.

2.5 Geometric optical model

The geometric optical model is based on the numerical integration of ray trajectory equation (2.2.4). Introducing augmented vector $\mathbf{z} = \begin{pmatrix} \mathbf{x} \\ \mathbf{u} \end{pmatrix}$ and denoting the right part of system (2.2.4) $\mathbf{F} = \begin{pmatrix} \mathbf{u} \\ n\nabla n(\mathbf{x}) \end{pmatrix}$, we can rewrite the ray trajectory equation as follows:

$$\dot{\mathbf{z}} = \mathbf{F}(\mathbf{z}) \tag{2.5.1}$$

We integrate this equation by means of the Runge - Kutta method of fifth order. This integration method, however, is not free of the difficulties connected with the accumulation of errors. As we shall see now, the accumulated errors can grow exponentially.

According to the definition of vector $\mathbf{u}$, its length must be equal to $n(\mathbf{x})$, and thus $\mathbf{u}^2/n^2 = 1$ must remain invariant during the integration of a ray. The initial condition must satisfy this restriction too. On the other hand, we can consider any solutions of this system with any initial conditions. We can derive the following dynamical equation:

$$\frac{d}{d\tau}\left(\frac{\mathbf{u}^2}{n^2}\right) = 2\frac{\langle \mathbf{u}, \nabla n\rangle}{n}\left(1 - \frac{\mathbf{u}^2}{n^2}\right) \tag{2.5.2}$$

which indicates that $\mathbf{u}^2/n^2$ is only invariant when it is equal to 1. Should it deviate from 1, $\mathbf{u}^2/n^2 - 1$ decreases or increases approximately exponentially when $\langle \mathbf{u}\nabla n\rangle$ is positive or negative respectively. For the raising part of the ray, where $\langle \mathbf{u}\nabla n\rangle < 0$, the discretization errors of the numerical integration scheme will thus rapidly increase.

In order to correct this, at each step of the standard Runge - Kutta method, we renorm vector $\mathbf{u}$. The numerical integration scheme is written as follows:

$$
\begin{aligned}
\mathbf{K}^1_{n-1} &= \mathbf{F}(\mathbf{z_{n-1}}) \\
\mathbf{K}^2_{n-1} &= \mathbf{F}(\mathbf{z_{n-1}} + \frac{\Delta\tau}{2}\mathbf{K}^1_{n-1}) \\
\mathbf{K}^3_{n-1} &= \mathbf{F}(\mathbf{z_{n-1}} + \frac{\Delta\tau}{2}\mathbf{K}^2_{n-1}) \\
\mathbf{K}^4_{n-1} &= \mathbf{F}(\mathbf{z_{n-1}} + \Delta\tau\mathbf{K}^3_{n-1}) \\
\mathbf{z'}_n &= \frac{\Delta\tau}{6}(\mathbf{K}^1_{n-1} + 2\mathbf{K}^2_{n-1} + 2\mathbf{K}^3_{n-1} + \mathbf{K}^4_{n-1}) + \mathbf{z_{n-1}} \\
\mathbf{z}_n &= \begin{pmatrix} \mathbf{x'_n} \\ n(\mathbf{x'_n})\mathbf{u'_n}/|\mathbf{u'_n}| \end{pmatrix}
\end{aligned}
\tag{2.5.3}
$$

Now we can describe the calculation of atmospheric refraction $\epsilon(p)$. For given GPS and LEO satellite positions and corresponding measurements of ϵ and p, we trace the ray starting at GPS with initial direction $\mathbf{u}_0$ approximately found from the impact parameter, the ray final point $\mathbf{z}_N$ being defined as that nearest to the LEO position. For the ray, we calculate the Doppler frequency shift:

$$
d = \frac{c - \mathbf{V}_{\mathrm{LEO}}\mathbf{u}_N}{c - \mathbf{V}_{\mathrm{GPS}}\mathbf{u}_0}\sqrt{\frac{c^2 - V^2_{\mathrm{GPS}}}{c^2 - V^2_{\mathrm{LEO}}}} - 1 \tag{2.5.4}
$$

which is used to find the refraction angle and impact parameter.

As was shown by Syndergaard (1997), a significant improvement of the accuracy of the Abel inversion is achieved, when the refraction angle and impact parameter are calculated in the coordinate frame of the center of the local curvature of the Earth surface, which allows for correction for ellipticity of the Earth's atmosphere. Although, at the first glance, it must not play an important role in 4DVar, in fact, it is useful also in this case, because it makes the calculated refraction angles and impact parameters more independent of the occultation geometry.

We shall now calculate the position of the local curvature center. Given an occultation point on the Earth's surface, the curvature of its normal cross-section with the occultation plane is calculated by means of Euler's theorem (Bronstein and Semendjajew, 1983):

$$
k_N = k_m \cos^2\theta + k_p \sin^2\theta \tag{2.5.5}
$$

where k_m and k_p are the main curvatures of the surface, in our case, meridional and parallel curvature respectively, and θ is the azimuth angle of the occultation plane direction, counted from the North. The main curvatures are calculated as follows:

$$
\begin{aligned}
k_m &= \frac{a_p a_e^4}{\left(a_e^4 + (a_p^2 - a_e^2)(x_1^2 + x_2^2)\right)^{3/2}} \\
k_p &= \frac{\cos\varphi}{\sqrt{x_1^2 + x_2^2}}
\end{aligned}
\tag{2.5.6}
$$

where we use both Cartesian coordinates $\mathbf{x} = (x_i)$ in the standard Earth frame and geodetic latitude φ of the point, a_e and a_p are the equatorial and polar semi-axes of the reference ellipsoid. The calculation of k_p was based on Meusnier's theorem (Bronstein and Semendjajew, 1983). The position of the local curvature center is then found as follows:

$$\mathbf{x}_{\mathrm{LC}} = \mathbf{x} - \frac{\mathbf{v}(\mathbf{x})}{k_N} \tag{2.5.7}$$

Calculation of the model refraction angle and impact parameter is then based on the solution of modified system (2.2.12) with respect to unknown unit vectors $\tilde{\mathbf{u}}_0$ and $\tilde{\mathbf{u}}_N$:

$$\begin{gathered} \frac{c - \mathbf{V}_{\mathrm{LEO}}\tilde{\mathbf{u}}_N}{c - \mathbf{V}_{\mathrm{GPS}}\tilde{\mathbf{u}}_0}\sqrt{\frac{c^2 - V_{\mathrm{GPS}}^2}{c^2 - V_{\mathrm{LEO}}^2}} - 1 = d \\ [(\mathbf{x}_0 - \mathbf{x}_{\mathrm{LC}}), \tilde{\mathbf{u}}_0] = [(\mathbf{x}_N - \mathbf{x}_{\mathrm{LC}}), \tilde{\mathbf{u}}_N] \end{gathered} \tag{2.5.8}$$

The system solved, the model refraction angle is defined as the angle between $\tilde{\mathbf{u}}_0$ and $\tilde{\mathbf{u}}_N$, the model impact parameter being equal to $\left| [(\mathbf{x}_0 - \mathbf{x}_{\mathrm{LC}}), \tilde{\mathbf{u}}_0] \right|$.

2.6 Linear tangent and linear adjoint models

We shall now describe the linear tangent model of the refraction, based on the geometric optical observation operator. We subdivide the linear tangent model into 3 parts: i) variations of the refractivity due to variations of the model parameters; ii) variations of the ray geometry due to variations of the refractivity; iii) variations of the refraction angles due to variations of the ray geometry. Such a subdivision allows for creation of a flexible code which can be easily modified for another Global Atmospheric Circulation Model, or for another ray-tracing technique, or for a different observation geometry.

2.6.1 Variations of refractivity

The first part of the linear tangent, which is also used in the linear adjoint model, describes the variations of the refractivity due to variations of the model parameters. Since the ray trajectory equations only include the combination $n\nabla n$, which in our model is assumed to be equal to $\mathbf{v}\langle \mathbf{v}, n\nabla n\rangle$, we only calculate the dependence of $\langle \mathbf{v}, n\nabla n\rangle$ on the model variables, i.e. derivatives:

$$\frac{\partial\langle \mathbf{v}(\mathbf{x}), n\nabla n(\mathbf{x})\rangle}{\partial(T_{ijk}, q_{ijk}, P_{s,jk})} \tag{2.6.1}$$

The corresponding variations are then calculated as follows:

$$\delta\langle \mathbf{v}(\mathbf{x}), n\nabla n(\mathbf{x})\rangle = \frac{\partial\langle \mathbf{v}(\mathbf{x}), n\nabla n(\mathbf{x})\rangle}{\partial(T_{ijk}, q_{ijk}, P_{s,jk})}\delta(T_{ijk}, q_{ijk}, P_{s,jk}) \tag{2.6.2}$$

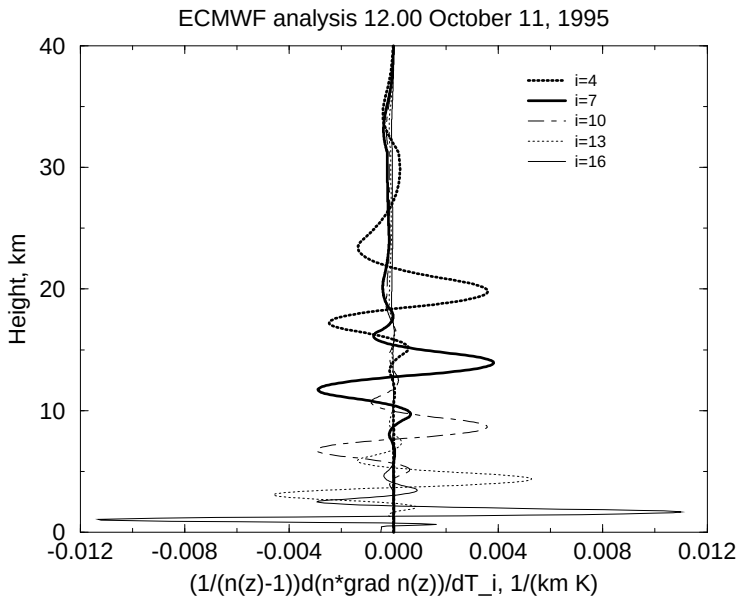

Figure 2: Vertical profiles of the sensitivity of $\langle \mathbf{v}, n\nabla n \rangle$ to variations of the temperature at model levels at 10N 20E.

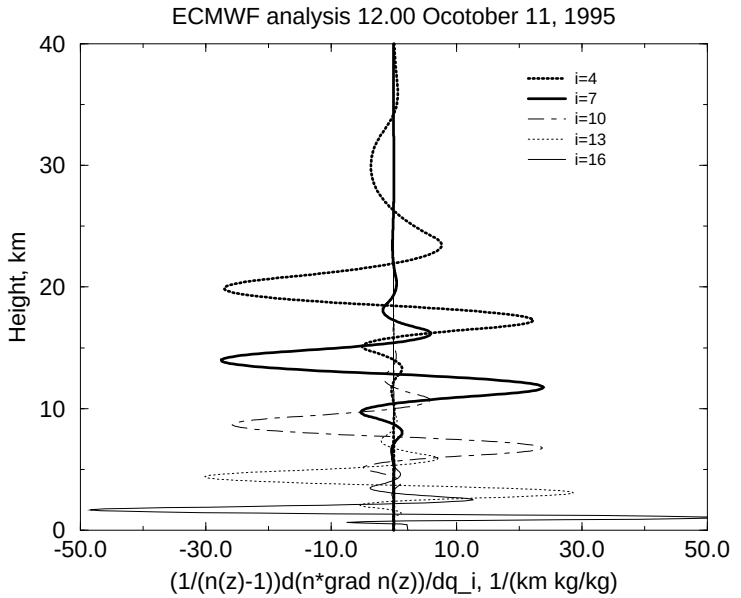

Figure 3: Vertical profiles of the sensitivity of $\langle \mathbf{v}, n\nabla n \rangle$ to variations of the humidity at model levels at 10N 20E.

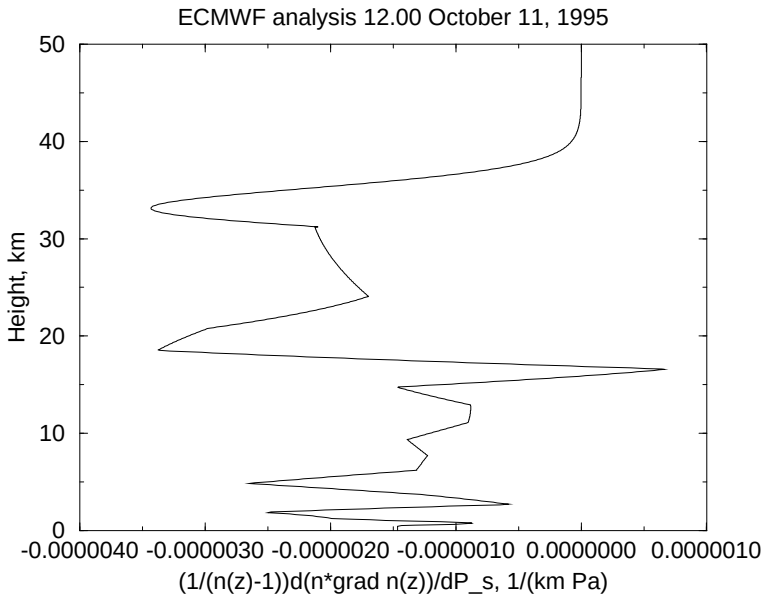

Figure 4: A vertical profile of the sensitivity of $\langle \mathbf{v}, n\nabla n \rangle$ to variations of the surface pressure at 10N 20E.

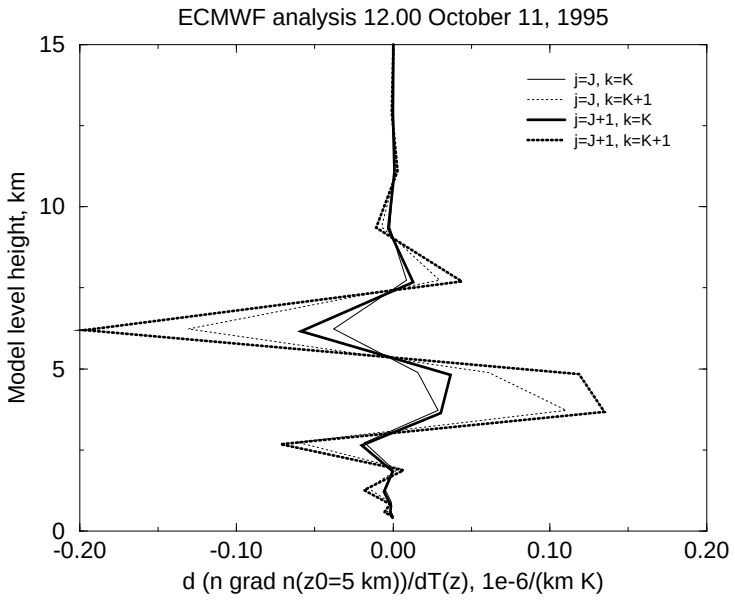

Figure 5: The sensitivity of $\langle \mathbf{v}, n\nabla n \rangle$ at a fixed height (5 km) to variations of the temperature at model levels i at 10N 20E.

We neglect the dependence of n that appears in the normalizing procedure defined in (2.5.3), on the variations of the model variables.

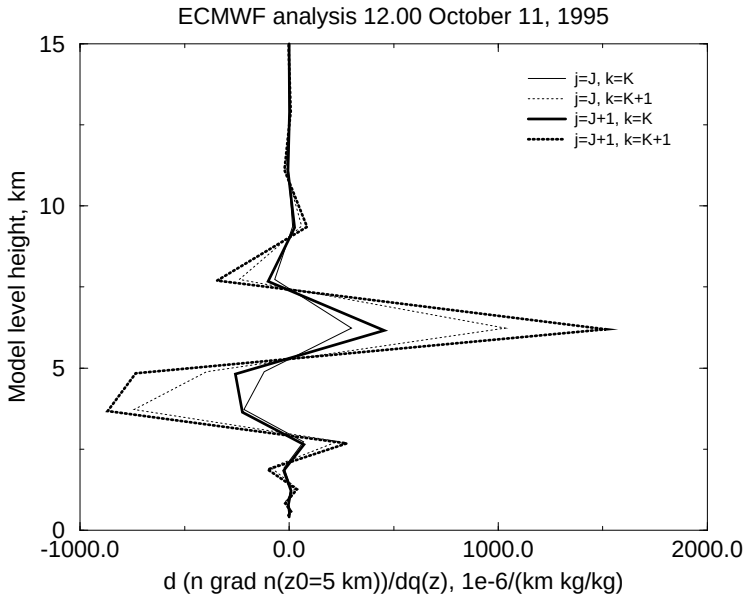

Figure 6: The sensitivity of $\langle \mathbf{v}, n\nabla n \rangle$ at a fixed height (5 km) to variations of the humidity at model levels i at 10N 20E.

The calculation of the derivatives is performed in the following steps:

1) Initialization. A pair of varied refractivity profiles for each positively and negatively varied model variable $(T_{ijk}, q_{ijk}, P_{s,jk})$ was calculated basing on formulas (2.3.1, 2.3.2). This calculation takes into account both variations of the gridded values of refractivity and variations of grid z_{ijk} defined by (2.3.3). The initialization was performed during the ray-tracing for the profiles influencing the ray only.

2) For a given spatial point $\mathbf{x}$ located at height z above the Earth's surface and projecting into horizontal grid mesh $(\varphi_J..\varphi_{J+1}, \lambda_K..\lambda_{K+1})$, derivatives

$$\frac{\partial N_{jk}(z)}{\partial(T_{ijk}, q_{ijk}, P_{s,jk})}, \frac{\partial N'_{jk}(z)}{\partial(T_{ijk}, q_{ijk}, P_{s,jk})}, \quad j = J..J+1, k = K..K+1 \tag{2.6.3}$$

are calculated using finite differences. Using the following interpolation formulas for $N(\mathbf{x}) = n(\mathbf{x}) - 1$ and $\langle \mathbf{v}(\mathbf{x}), \nabla N(\mathbf{x}) \rangle = N'_z(\mathbf{x})$:

$$N(\mathbf{x}) = \exp\left(\sum_{j=J}^{J+1}\sum_{k=K}^{K+1} \beta_{jk} \ln N_{jk}(z)\right)$$
$$N'_z(\mathbf{x}) = N(\mathbf{x}) \sum_{j=J}^{J+1}\sum_{k=K}^{K+1} \beta_{jk} \frac{N'_{jk}(z)}{N_{jk}(z)} \tag{2.6.4}$$

where β_{jk} are the coefficients of the linear interpolation with respect to latitude and longitude, we can find the derivatives of $\langle \mathbf{v}(\mathbf{x}), n\nabla n(\mathbf{x})\rangle$:

$$\frac{\partial\langle \mathbf{v}(\mathbf{x}), n\nabla n(\mathbf{x})\rangle}{\partial(T_{ijk}, q_{ijk}, P_{s,jk})} = \sum_{j=J}^{J+1}\sum_{k=K}^{K+1}\beta_{jk}\left\{\frac{N(\mathbf{x})N'_z(\mathbf{x})}{N_{jk}(z)}\frac{\partial N_{jk}(z)}{\partial(T_{ijk}, q_{ijk}, P_{s,jk})}+\right.$$
$$+(1+N(\mathbf{x}))\left[\frac{N'_z(\mathbf{x})}{N_{jk}(z)} - \frac{N(\mathbf{x})N'_{jk}(z)}{N^2_{jk}(z)}\right]\frac{\partial N_{jk}(z)}{\partial(T_{ijk}, q_{ijk}, P_{s,jk})}+$$
$$\left.+\frac{(1+N(\mathbf{x}))N'_z(\mathbf{x})}{N_{jk}(z)}\frac{\partial N'_{jk}(z)}{\partial(T_{ijk}, q_{ijk}, P_{s,jk})}\right\} \tag{2.6.5}$$

Figures 2, 3, and 4 give a few examples of the calculation of derivatives $\dfrac{\partial\langle \mathbf{v}(\mathbf{x}), n\nabla n(\mathbf{x})\rangle}{\partial(T_{ijk}, q_{ijk}, P_{s,jk})}$ as functions of height z of point $\mathbf{x}$ for different numbers i of the model level for fixed latitude and longitude indexes j, k. The derivatives are normed to the refractivity.

Figures 5 and 6 show derivatives $\dfrac{\partial\langle \mathbf{v}(\mathbf{x}), n\nabla n(\mathbf{x})\rangle}{\partial(T_{ijk}, q_{ijk})}$ at a fixed height of 5 km as functions of model level heights z_i for the four corners of the horizontal grid mesh containing the projection of $\mathbf{x}$.

2.6.2 Variations of ray geometry

We shall now consider variations of the ray geometry due to variations of $\langle \mathbf{v}, n\nabla n\rangle$.

At the n-th step of the numerical integration of the ray trajectory equation, the calculation of $\mathbf{z}_n$ depends on the values of right part $\mathbf{F}$ in points $\mathbf{z}^\mu_{n-1}$, $\mu = 1..4$:

$$\begin{aligned}
\mathbf{z}^1_{n-1} &= \mathbf{z}_{n-1}\\
\mathbf{z}^2_{n-1} &= \mathbf{z}_{n-1} + \frac{\Delta\tau}{2}\mathbf{K}^1_{n-1}\\
\mathbf{z}^3_{n-1} &= \mathbf{z}_{n-1} + \frac{\Delta\tau}{2}\mathbf{K}^2_{n-1}\\
\mathbf{z}^4_{n-1} &= \mathbf{z}_{n-1} + \Delta\tau\mathbf{K}^3_{n-1}
\end{aligned} \tag{2.6.6}$$

where $\mathbf{K}^\mu_{n-1}$ are defined in (2.5.3). Remembering definition (2.2.4), (2.5.1) of $\mathbf{F}(\mathbf{z})$, we can express its operator derivatives as follows:

$$\hat{\mathbf{B}}^\mu_n \equiv \left.\frac{\partial\mathbf{F}(\mathbf{z})}{\partial\mathbf{z}}\right|_{\mathbf{z}=\mathbf{z}^\mu_{n-1}} = \begin{pmatrix} \hat{\mathbf{0}} & \hat{\mathbf{I}} \\ \nabla\otimes\nabla n^2(\mathbf{x}^\mu_{n-1})/2 & \hat{\mathbf{0}}\end{pmatrix} \approx \begin{pmatrix} \hat{\mathbf{0}} & \hat{\mathbf{I}} \\ \nabla\otimes\nabla n(\mathbf{x}^\mu_{n-1}) & \hat{\mathbf{0}}\end{pmatrix} \tag{2.6.7}$$

where $\hat{\mathbf{0}}$ and $\hat{\mathbf{I}}$ are the zero and unit matrices of dimension 3×3.

Introducing variations $\bar{\delta}\mathbf{F}^\mu_{n-1}$ of the form of the right part due to variations of the model refractivity, we can derive the following expression for variations of $\mathbf{z}'_n$:

$$
\begin{aligned}
\delta\mathbf{z}'_n = \Bigg[\hat{\mathbf{I}} + \frac{\Delta\tau}{6}\left(\hat{\mathbf{B}}^1_n + 2\hat{\mathbf{B}}^2_n + 2\hat{\mathbf{B}}^3_n + \hat{\mathbf{B}}^4_n\right) + \\
+\frac{\Delta\tau^2}{6}\left(\hat{\mathbf{B}}^2_n\hat{\mathbf{B}}^1_n + \hat{\mathbf{B}}^3_n\hat{\mathbf{B}}^2_n + \hat{\mathbf{B}}^4_n\hat{\mathbf{B}}^3_n\right) + \\
+\frac{\Delta\tau^3}{12}\left(\hat{\mathbf{B}}^3_n\hat{\mathbf{B}}^2_n\hat{\mathbf{B}}^1_n + \hat{\mathbf{B}}^4_n\hat{\mathbf{B}}^3_n\hat{\mathbf{B}}^2_n\right) + \\
+\frac{\Delta\tau^4}{24}\hat{\mathbf{B}}^4_n\hat{\mathbf{B}}^3_n\hat{\mathbf{B}}^2_n\hat{\mathbf{B}}^1_n\Bigg]\,\delta\mathbf{z}_{n-1} + \\
+\left(\frac{\Delta\tau}{6}\hat{\mathbf{I}} + \frac{\Delta\tau^2}{6}\hat{\mathbf{B}}^2_n + \frac{\Delta\tau^3}{12}\hat{\mathbf{B}}^3_n\hat{\mathbf{B}}^2_n + \frac{\Delta\tau^4}{24}\hat{\mathbf{B}}^4_n\hat{\mathbf{B}}^3_n\hat{\mathbf{B}}^2_n\right)\bar{\delta}\mathbf{F}^1_{n-1} + \\
+\left(\frac{\Delta\tau}{3}\hat{\mathbf{I}} + \frac{\Delta\tau^2}{6}\hat{\mathbf{B}}^3_n + \frac{\Delta\tau^3}{12}\hat{\mathbf{B}}^4_n\hat{\mathbf{B}}^4_n\right)\bar{\delta}\mathbf{F}^2_{n-1} + \\
+\left(\frac{\Delta\tau}{3}\hat{\mathbf{I}} + \frac{\Delta\tau^2}{6}\hat{\mathbf{B}}^4_n\right)\bar{\delta}\mathbf{F}^3_{n-1} + \\
+\frac{\Delta\tau}{6}\hat{\mathbf{I}}\bar{\delta}\mathbf{F}^4_{n-1} \equiv \\
\equiv \hat{\mathbf{B}}'_n\delta\mathbf{z}_{n-1} + \sum_\mu \hat{\mathbf{C}}^\mu_n\bar{\delta}\mathbf{F}^\mu_{n-1}
\end{aligned}
\tag{2.6.8}
$$

where the last line is the definition of matrices $\hat{\mathbf{B}}'_n$ and $\hat{\mathbf{C}}^\mu_n$, and $\hat{\mathbf{I}}$ is the unit matrix of dimension 6×6.

Introducing notation $\alpha^\mu_{n-1} = \langle \mathbf{v}(\mathbf{x}^\mu_{n-1}), n\nabla n(\mathbf{x}^\mu_{n-1})\rangle$ for the parameters influencing the ray geometry, and uniting parameters α^μ_{n-1} into vector $\mathbf{a}_{n-1}$, we can write the expression for the variations of the form of the right part:

$$
\bar{\delta}\mathbf{F}^\mu_{n-1} = \hat{\mathbf{A}}^\mu_n\delta\mathbf{a}_{n-1} \tag{2.6.9}
$$

where the matrices $\hat{\mathbf{A}}^\mu$ are defined as follows:

$$
\begin{aligned}
\hat{\mathbf{A}}^1_n &= \begin{pmatrix} \mathbf{0} & \mathbf{0} & \mathbf{0} & \mathbf{0} \\ \mathbf{v}(\mathbf{x}^1_{n-1}) & \mathbf{0} & \mathbf{0} & \mathbf{0} \end{pmatrix}, \quad \hat{\mathbf{A}}^2_n = \begin{pmatrix} \mathbf{0} & \mathbf{0} & \mathbf{0} & \mathbf{0} \\ \mathbf{0} & \mathbf{v}(\mathbf{x}^2_{n-1}) & \mathbf{0} & \mathbf{0} \end{pmatrix} \\
\hat{\mathbf{A}}^3_n &= \begin{pmatrix} \mathbf{0} & \mathbf{0} & \mathbf{0} & \mathbf{0} \\ \mathbf{0} & \mathbf{0} & \mathbf{v}(\mathbf{x}^3_{n-1}) & \mathbf{0} \end{pmatrix}, \quad \hat{\mathbf{A}}^4_n = \begin{pmatrix} \mathbf{0} & \mathbf{0} & \mathbf{0} & \mathbf{0} \\ \mathbf{0} & \mathbf{0} & \mathbf{0} & \mathbf{v}(\mathbf{x}^4_{n-1}) \end{pmatrix}
\end{aligned}
\tag{2.6.10}
$$

where $\mathbf{0}$ is the zero (column) vector.

The last remaining operation to be considered is the normalization of vector $\mathbf{u}'_n$:

$$
\mathbf{u}_n = \frac{\mathbf{u}'_n n(\mathbf{x}'_n)}{|\mathbf{u}'_n|} \tag{2.6.11}
$$

For infinitesimal variation $\delta\mathbf{u}_n$, we have the following expression:

$$
\delta\mathbf{u}_n = \langle\nabla n(\mathbf{x}'_n), \delta\mathbf{x}'_n\rangle\frac{\mathbf{u}'_n}{|\mathbf{u}'_n|} + n(\mathbf{x}'_n)\left[\frac{\delta\mathbf{u}'_n}{|\mathbf{u}'_n|} - \frac{\mathbf{u}'_n(\mathbf{u}'_n, \delta\mathbf{u}'_n)}{\mathbf{u}'^2_n}\right] \tag{2.6.12}
$$

Returning to the variation of the augmented vector $\mathbf{z}$, we can rewrite this in matrix form as follows:

$$\delta\mathbf{z}_n = \hat{\mathbf{R}}_n \delta\mathbf{z}'_n \tag{2.6.13}$$

with the following definition of matrix $\hat{\mathbf{R}}_n$:

$$\hat{\mathbf{R}}_n = \begin{pmatrix} \hat{\mathbf{I}} & \hat{\mathbf{0}} \\ \dfrac{\mathbf{u}'_n \otimes \nabla n(\mathbf{x}'_n)}{|\mathbf{u}'_n|} & \dfrac{n(\mathbf{x}'_n)}{|\mathbf{u}'_n|}\left(\hat{\mathbf{I}} - \dfrac{\mathbf{u}'_n \otimes \mathbf{u}'_n}{|\mathbf{u}'_n|}\right) \end{pmatrix} \tag{2.6.14}$$

where $\hat{\mathbf{I}}$ and $\hat{\mathbf{0}}$ are the unit and zero matrices of dimension 3×3, respectively.

Collecting all the transformations described above, we arrive at the equation for variations of the augmented vector $\mathbf{z}$:

$$\begin{aligned} \delta\mathbf{z}_n = \hat{\mathbf{R}}_n \hat{\mathbf{B}}'_n \delta\mathbf{z}_{n-1} + \hat{\mathbf{R}}_n \sum_\mu \hat{\mathbf{C}}^\mu_n \hat{\mathbf{A}}^\mu_n \delta\mathbf{a}_{n-1} \equiv \\ \equiv \hat{\mathbf{B}}_n \delta\mathbf{z}_{n-1} + \hat{\mathbf{C}}_n \delta\mathbf{a}_{n-1} \end{aligned} \tag{2.6.15}$$

2.6.3 Variations of refraction angle

The refraction angle and impact parameter are functions of the initial and final conditions of a ray trajectory, as defined by equations (2.5.4), (2.5.8):

$$\begin{aligned} \epsilon &= \epsilon(\mathbf{z}_0, \mathbf{z}_N) \\ p &= p(\mathbf{z}_0, \mathbf{z}_N) \end{aligned} \tag{2.6.16}$$

The final condition $\mathbf{z}_N$ is a function of the initial condition and the parameters:

$$\mathbf{z}_N = \mathbf{z}_N(\mathbf{z}_0, \mathbf{a}) \tag{2.6.17}$$

where $\mathbf{a}$ is the complete vector of parameters α^μ_n. The full variations of the refraction angle and impact parameter can be written in the following form:

$$\begin{aligned} \delta\epsilon &= \frac{\partial\epsilon}{\partial\mathbf{z}_0}\delta\mathbf{z}_0 + \frac{\partial\epsilon}{\partial\mathbf{z}_N}\frac{\partial\mathbf{z}_N}{\partial\mathbf{z}_0}\delta\mathbf{z}_0 + \frac{\partial\epsilon}{\partial\mathbf{z}_N}\frac{\partial\mathbf{z}_N}{\partial\mathbf{a}}\delta\mathbf{a} \\ \delta p &= \frac{\partial p}{\partial\mathbf{z}_0}\delta\mathbf{z}_0 + \frac{\partial p}{\partial\mathbf{z}_N}\frac{\partial\mathbf{z}_N}{\partial\mathbf{z}_0}\delta\mathbf{z}_0 + \frac{\partial p}{\partial\mathbf{z}_N}\frac{\partial\mathbf{z}_N}{\partial\mathbf{a}}\delta\mathbf{a} \end{aligned} \tag{2.6.18}$$

We need the variation of the refraction angle with a given impact parameter, so we choose the variation of the initial condition so that δp should be equal to 0. In order to arrive at

a completely defined system of conditions for $\delta\mathbf{z}_0$, we assume that it is sufficient to vary ray direction $\mathbf{u}_0$ only, and that its variation is coplanar with vectors $\mathbf{x}_0$ and $\mathbf{x}_N$. Complementing this with the requirement for varied $\mathbf{u}_0$ to remain a unit vector, we can uniquely define $\delta\mathbf{z}_0$ from the following system:

$$\begin{gathered}\left(\frac{\partial p}{\partial \mathbf{z}_0}+\frac{\partial p}{\partial \mathbf{z}_N}\frac{\partial \mathbf{z}_N}{\partial \mathbf{z}_0}\right)\delta\mathbf{z}_0=-\frac{\partial p}{\partial \mathbf{z}_N}\frac{\partial \mathbf{z}_N}{\partial \mathbf{a}}\delta\mathbf{a}\\ \delta\mathbf{x}_0=0\\ (\delta\mathbf{u}_0,[\mathbf{x}_0,\mathbf{x}_N])=0\\ (\mathbf{u}_0,\delta\mathbf{u}_0)=0\end{gathered} \tag{2.6.19}$$

We shall use the following notation for the solution of this system:

$$\delta\mathbf{z}_0=-\frac{d\mathbf{z}_0}{dp}\frac{\partial p}{\partial \mathbf{z}_N}\frac{\partial \mathbf{z}_N}{\partial \mathbf{a}}\delta\mathbf{a} \tag{2.6.20}$$

For the variation of the refraction angle, we can write the following expression:

$$\delta\epsilon=\left[\frac{\partial\epsilon}{\partial \mathbf{z}_N}-\left(\frac{\partial\epsilon}{\partial \mathbf{z}_0}+\frac{\partial\epsilon}{\partial \mathbf{z}_N}\frac{\partial \mathbf{z}_N}{\partial \mathbf{z}_0}\right)\frac{d\mathbf{z}_0}{dp}\frac{\partial p}{\partial \mathbf{z}_N}\right]\frac{\partial \mathbf{z}_N}{\partial \mathbf{a}}\delta\mathbf{a}\equiv\frac{d\epsilon}{d\mathbf{z}_N}\frac{\partial \mathbf{z}_N}{\partial \mathbf{a}}\delta\mathbf{a} \tag{2.6.21}$$

The full derivative $\dfrac{d\epsilon}{d\mathbf{z}_N}$ introduced here, describes the sensitivity of the refraction angle with respect to the ray geometry.

2.6.4 Linear adjoint model

Now we have everything to be able to find the derivative of the refraction angle with respect to the model variables:

$$\frac{\partial\epsilon(p)}{\partial(T_{ijk},q_{ijk},P_{s,jk})}=\frac{d\epsilon}{d\mathbf{z}_N}\frac{\partial \mathbf{z}_N}{\partial \mathbf{a}}\frac{\partial \mathbf{a}}{\partial(T_{ijk},q_{ijk},P_{s,jk})} \tag{2.6.22}$$

The derivatives $\dfrac{d\epsilon}{d\mathbf{z}_N}$ and $\dfrac{\partial \mathbf{a}}{\partial(T_{ijk},q_{ijk},P_{jk})}$ have already been found, and we need now $\dfrac{\partial \mathbf{z}_N}{\partial \mathbf{a}}$ and $\dfrac{\partial \mathbf{z}_N}{\partial \mathbf{z}_0}$ (the latter is included into the definition of $\dfrac{d\epsilon}{d\mathbf{z}_N}$). Using (2.6.15), it is easy to derive the following expressions:

$$\begin{aligned}\frac{\partial \mathbf{z}_N}{\partial \mathbf{z}_0} &= \hat{\mathbf{B}}_N\hat{\mathbf{B}}_{N-1}...\hat{\mathbf{B}}_1\\ \frac{\partial \mathbf{z}_N}{\partial \mathbf{a}_{n-1}} &= \hat{\mathbf{B}}_N\hat{\mathbf{B}}_{N-1}...\hat{\mathbf{B}}_{n+1}\hat{\mathbf{C}}_n\end{aligned} \tag{2.6.23}$$

Figure 7 shows an example of the refraction angle profile observed in a radio occultation and the results of the application of our observation operator to the global fields from an

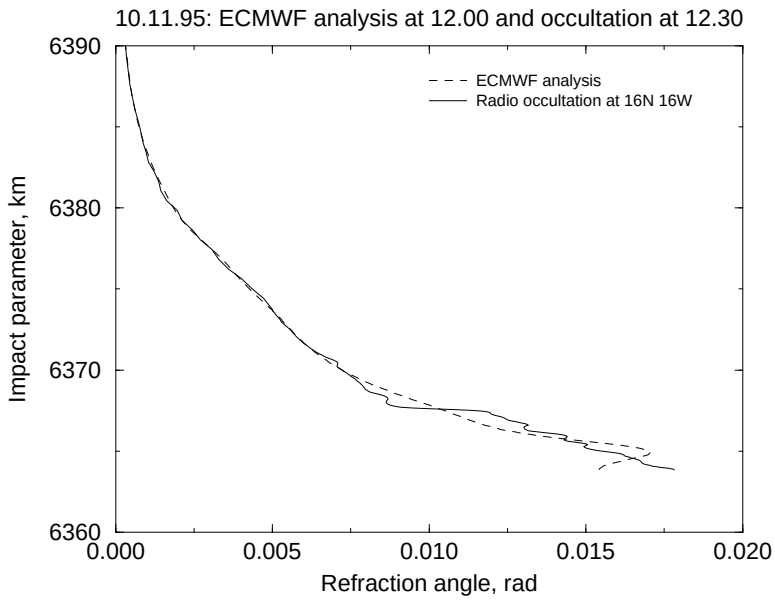

Figure 7: A comparison of the observed refraction angle with its computation for the global field from an ECMWF analysis: an occultation at 16N 16W.

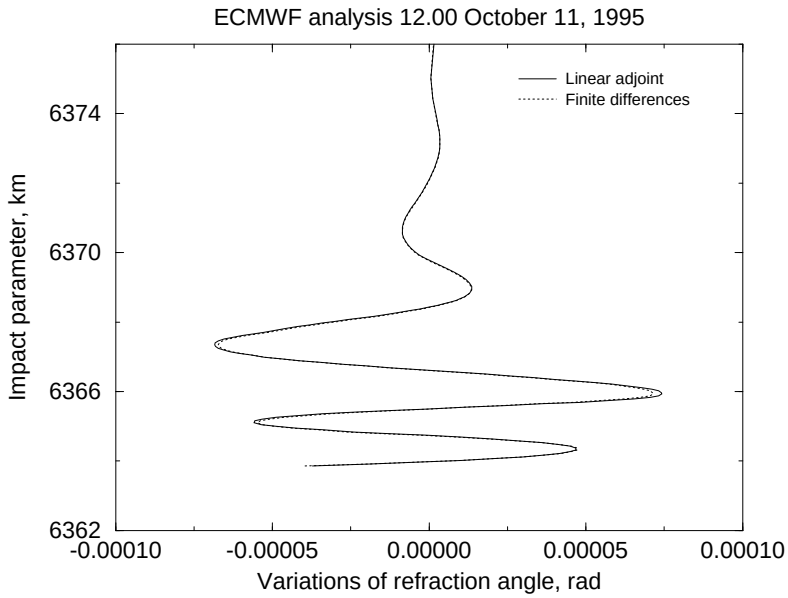

Figure 8: The variations of the refraction angle due to random variations of the model variables: a simulated occultation at 16N 16W with the same geometry as in Figure 7.

ECMWF analysis, i.e. the computation of the refraction angle for a simulated sounding with the same geometry. Figure 8 shows the variations of the profile of the refraction angle with random variations of the model variable. The result of application of the tangent linear model is compared with the reference computation based on the finite difference method. The comparison indicates a very good agreement of both computations.

3 Conclusion

In this report, we have considered the principles of 3D/4DVar of the refractometric data. The basic requirements of the 3D/4DVar for any kind of the data to be assimilated into a Numerical Weather Prediction Model are as follows. It is necessary to have i) the observation operator, i.e. an algorithm that maps the model variables representing the atmospheric state to the observables; ii) the linear tangent model, i.e. the Fréchet derivative of the observation operator, describing the first order variations of the observables with respect to variations of the model variables; iii) the tangent linear model that is capable of calculating the derivatives of the observables with respect to the model variables.

Although the necessity of 3D/4DVar of the refractometric data has been recognized long ago, it has proved to be difficult to implement this assimilation scheme for the refractometric measurements. The basic difficulty consisted in the refractometric measurements representing some complicated nonlinear functionals of the atmospheric state. But now it is possible to affirm that this difficulty has been overcome. In this report we describe a package of the algorithms that enables 3D/4DVar of GNSS radio occultaion data.

Based on the physical model of the occultation experiment, we have designed its numerical model, i.e. the observation operator. This additionally requires a model of a smooth 3D distribution of the atmospheric refractivity. The model of the atmospheric refractivity is based on some interpolation of its gridded field, calculated from the fields of the model variables. Although the model ECHAM3 operates with the concept of the spherical Earth, for assimilation of the real data, its variables must be related to the reference ellipsoid which is also included into the refractivity model.

The mathematical analysis of the observation operator allowes for derivation of both linear tangent and linear adjoint models. The models were subdivided into three blocks: i) refractivity; ii) ray geometry; iii) refraction measurements. Such a subdivision allowes for creation of a flexible code that can easily be modified for another atmospheric model, or another ray-tracing technique, or another observation geometry.

All these numerical models are complemented with a program for the primary processing of the radio occultation data. The following algorithms are included: i) the canonical transform processing that allows for handling of the tropospheric data where the multipath propagation effects are significant; ii) data filtering (standard Fourier filtering is used); iii) derivation of the refraction angle from the Doppler shift (an improved numerical algorithm was designed); iv) ionospheric correction of the refraction angle (we use the standard method of the linear combination of the refraction angles).

All the algorithms exist in the form of a working program code. Being implemented with an interface for their interaction with the standard 4DVar algorithms, they can be used in a system of operational data assimilation.

References

Anthes, R., Exner, M., Rocken, C. and Ware, R. (1997): *Results from the GPS/MET experiment and potential applications to gewex*. GEWEX News, **7**, 3–6.

Bean, B. R. and Datton, E. J. (1968): *Radio meteorology*. Dover Publ. Inc., New-York.

Bronstein, I. N. and Semendjajew, K. A. (1983): *Taschenbuch der Mathematik*. B. G. Teubner Verlaggesellschaft, Leipzig.

COSPAR (1986): *COSPAR international reference atmosphere*. Pergamon Press, Oxford, New-York, 1st edn..

DKRZ (1994): *The ECHAM3 atmospheric general circulation model*. Technical Report No. 6, Modelbetreuungsgruppe, Hamburg.

Eyre, J. R. (1994): *Assimilation of radio occultation measurements into a numerical weather prediction system*. Technical Memorandum No. 199, European Center for Medium-Range Weather Forecast.

Fjeldbo, G. and Eshleman, V. R. (1968): *The atmosphere of Mars analyzed by integral inversion of the Mariner iv occultation data*. Planetary and Space Science, **16**, 123–140.

Gorbunov, M. E. (1990): *Solution of the inverse problems of remote atmospheric refractometry on limb paths*. Izvestiya Academy of Sciences SSSR, Atmospheric and Oceanic Physics, English Translation, **26, no. 2**, 86–91.

Gorbunov, M. E., Gurvich, A. S. and Bengtsson, L. (1996b): *Advanced algorithms of inversion of GPS/MET satellite data and their application to reconstruction of temperature and humidity*. Report No. 211, Max-Planck Institute for Meteorology, Hamburg.

Gorbunov, M. E. and Sokolovskiy, S. V. (1993): *Remote sensing of refractivity from space for global observations of atmospheric parameters*. Report No. 119, Max-Planck Institute for Meteorology, Hamburg.

Gorbunov, M. E., Sokolovskiy, S. V. and Bengtsson, L. (1996a): *Space refractive tomography of the atmosphere: modeling of direct and inverse problems*. Report No. 210, Max-Planck Institute for Meteorology, Hamburg.

Gurvich, A. S. and Krasil'nikova, T. G. (In Russian 1987, In English 1990): *Navigation satellites for radio sensing of the Earth's atmosphere*. Soviet Journal of Remote Sensing, **7, no. 6**, 1124–1131.

Hocke, K. (1997): *Inversion of GPS meteorology data*. Annales Geophysicae, **15, no. 4**, 443–450.

Hoffman, R. N., Louis, J.-F. and Nehrkorn, T. (1992): *A method for implementing adjoint calculations in the discrete case*. Technical Memorandum No. 184, European Center for Medium-Range Weather Forecast.

Kliore, A. J., Cain, D. L., Levy, G. S., Eshleman, V. R., Fjeldbo, G. and Drake, F. D. (1965): *Occultation experiment: Results of the first direct measurement of Mars' atmosphere and ionosphere*. Science, **149**, 1243–1248.

Kravtsov, Y. A. and Orlov, Y. I. (1990): *Geometrical optics of inhomogeneous media*. Springer, Berlin.

Kuo, Y.-H., Zou, X., Chen, S.-J., Huang, W., Guo, Y.-R., Anthes, R., Exner, M., Hunt, D., Rocken, C. and Reed, R. (1997): *Sounding through an intense upper level front*. Bulletin of American Meteorological Society, accepted for publication.

Kursinski, E. R., Hajj, G. A., Bertiger, W. I., Leroy, S. S., Meehan, T. K., Romans, L. J., Schofield, J. T., McCleese, D. J., Melbourne, W. G., Thornton, C. L., Yunck, T. P., Eyre, J. R. and Nagatani, R. N. (1996): *Initial results of radio occultation observation of Earth's atmosphere using the global positioning system*. Science, **271**, 1107–1110.

Lambeck, K. (1988): *Geophysical geodesy: the slow deformation of the Earth*. Clarendon press, Oxford.

Lindal, G. F. (1992): *The atmosphere of Neptune: An analysis of radio occultation data acquired with Voyager*. Astronomical Journal, **103**, 967–982.

Lindal, G. F., Lyons, J. R., Sweetnam, D. N., Eshleman, V. R., Hinson, D. P. and Tyler, G. L. (1990): *The atmosphere of Neptune: Results of radio occultation measurements with the Voyager 2 spacecraft*. Geophysical Research Letters, **17**, 1733–1736.

List, R. J., ed. (1968): *Acceleration of gravity, Smithsonian Meteorological Tables*. Smithsonian Institution, Washington D. C., 6th edn..

Liu, H., Zou, X., Shao, H., Anthes, R. A., Chang, J. C., Tseng, J. H. and Wang, B. (2001): *Impact of 837 GPS/MET bending angle profiles on assimilation and forecasts for the period June 20-30, 1995*. J. Geophys. Res., **106, no. D23**, 31771–31786.

Liu, H. and Zou, X. (2003): *Improvements to a GPS radio occultation ray-tracing model and their impacts on assimilation of bending angle*. J. Geophys. Res., **108, no. D17**, 4548, doi: 10.1029/2002JD003160.

Lusignan, B., Modrell, G., Morrison, A., Pomalaza, J. and Ungar, S. G. (1969): *Sensing of the Earth's atmosphere with occultation satellites*. Proceedings of IEEE, **57**, 458–467.

Martin, J. (1992): *Simulation of wave propagation in random media: theory and applications*. In: *Wave propagation in random media (scintillations)*, edited by Tatarskii, V. I., Ishimaru, A. and Zavorotny, V. U., Bellingham, Washington USA, Bristol and Philadelphia. SPIE - The International Society for Optical Engineering and Institute of Physics Publishing.

Melbourne, W. G., Yunck, T. P., Young, L. E., Hager, B. H., Lindal, G. F. and and. G. H. Born, C. H. L. (1988): *GPS geoscience instrument for EOS and Space Station*. JPL Proposal to NASA AO OSSA-1-88, JPL.

Melbourne, W. G., Davis, E. S., Duncan, C. B., Hajj, G. A., Hardy, K. R., Kursinski, E. R., Meehan, T. K. and Young, L. E. (1994): *The application of spaceborne GPS to atmospheric limb sounding and global change monitoring*. JPL Publ. 94-18, Jet Propul. Lab., Pasadena Calif.

NOAA (1976): *U. S. Standard Atmosphere*. NOAA and NASA and USAF, Washington D. C.

Phinney, R. A. and Anderson, D. L. (1968): *On the radio occultation method for studying planetary atmospheres*. Journal of Geophysical Research, **73**, 1819–1827.

Rangaswamy, S. (1976): *Recovery of atmospheric parameters from the APOLLO/SOYUZ-ATS-F radio occultation data*. Geophysical Research Letters, **8**, 483–486.

Rocken, C., Anthes, R., Exner, M., Hunt, D., Sokolovsky, S., Ware, R., Gorbunov, M., Schreiner, W., Feng, D., Herman, B., Kuo, Y.-H. and Zou, X. (1997): *Verification of GPS/MET data in the neutral atmosphere*. Journal of Geophysical Research, submitted.

Sokolovskiy, S. V. (1990): *Solution of the inverse refraction problem by sensing of the atmosphere from space*. Soviet Journal of Remote Sensing, **3**, 333–338.

Syndergaard, S. (1997): *Modeling the impact of the Earth's oblateness on the retrieval of temperature and pressure profiles from limb sounding*. Journal of Atmospheric and Solar-Terrestrial Physics, accepted for publication.

Syndergaard, S. and Høeg, P. (1996): *Realistic radio occultation simulations using a 3d ray tracing model and subsequent inversion with the Abel transform*. In: *URSI GPS/MET Workshop*, Tucson, Arizona.

Tatarskii, V. I. (1961): *Wave propagation in a turbulent medium*. MacGraw-Hill, New York.

Tatarskii, V. I. (1968): *Determining atmospheric density from satellite phase and refraction angle measurements*. Izvestiya Academy of Sciences SSSR, Atmospheric and Oceanic Physics, English Translation, **4, no. 7**, 401–406.

Vorob'ev, V. V. and Krasil'nikova, T. G. (1994): *Estimation of the accuracy of the atmospheric refractive index recovery from Doppler shift measurements at frequencies used in the NAVSTAR system*. Izvestiya Academy of Sciences SSSR, Atmospheric and Oceanic Physics, English Translation, **29, no. 5**, 602–609.

Ware, R., Exner, M., Feng, D., Gorbunov, M., Hardy, K., Herman, B., Kuo, Y.-H., Meehan, T., Melbourne, W., Rocken, C., Schreiner, W., Sokolovsky, S., Solheim, F., Zou, X., Anthes, R., Businger, S. and Trenberth, K. (1996): *GPS*

sounding of the atmosphere from Low Earth Orbit: Preliminary results. Bulletin of the American Meteorological Society, **77, no. 1**, 19–40.

Weng Cho Chew (1994): *Waves and fields in inhomogeneous media*. IEEE press, New York.

Yakovlev, O. I., Matyugov, S. S. and Vilkov, I. A. (1995): *Attenuation and scintillation of radio waves in the Earth's atmosphere from radio occultation experiment on satellite-to-satellite links*. Radio Science, **30, no. 3**, 591–602.

Zou, X., Wang, B., H. Liu, R. A. A., Matsumura, T. and Zhu, Y. J. (2000): *Use of GPS/MET refraction angles in three-dimensional variational analysis*. Quart. J. Royal Meteor. Soc., **126, no. 570**, 3013–3040.

Zou, X., Kuo, Y.-H. and Guo, Y.-R. (1995): *Assimilation of atmospheric radio refractivity using a nonhydrostatic adjoint model*. Monthly Weather Review, **123**, 2229–2249.

Zverev, V. A. (1975): *Radio-optics*. Soviet Radio, Moscow.

MPI-Report-Reference: *Reprinted in

Report 1 - 302 Please order the reference list from MPI for Meteorology, Hamburg

Report No. 303
December 1999
The leading variability mode of the coupled troposphere-stratosphere winter circulation in different climate regimes
Judith Perlwitz, Hans-F. Graf, Reinhard Voss
* Journal of Geophysical Research, 105, 6915-6926, 2000

Report No. 304
January 2000
Generation of SST anomalies in the midlatitudes
Dietmar Dommenget, Mojib Latif
* Journal of Climate, 1999 (submitted)

Report No. 305
June 2000
Tropical Pacific/Atlantic Ocean Interactions at Multi-Decadal Time Scales
Mojib Latif
* Geophysical Research Letters, 28,3,539-542,2001

Report No. 306
June 2000
On the Interpretation of Climate Change in the Tropical Pacific
Mojib Latif
* Journal of Climate, 2000 (submitted)

Report No. 307
June 2000
Observed historical discharge data from major rivers for climate model validation
Lydia Dümenil Gates, Stefan Hagemann, Claudia Golz

Report No. 308
July 2000
Atmospheric Correction of Colour Images of Case I Waters - a Review of Case II Waters - a Review
D. Pozdnyakov, S. Bakan, H. Grassl
* Remote Sensing of Environment, 2000 (submitted)

Report No. 309
August 2000
A Cautionary Note on the Interpretation of EOFs
Dietmar Dommenget, Mojib Latif
* Journal of Climate, 2000 (submitted)

Report No. 310
September 2000
Midlatitude Forcing Mechanisms for Glacier Mass Balance Investigated Using General Circulation Models
Bernhard K. Reichert, Lennart Bengtsson, Johannes Oerlemans
* Journal of Climate, 2000 (accepted)

Report No. 311
October 2000
The impact of a downslope water-transport parameterization in a global ocean general circulation model
Stephanie Legutke, Ernst Maier-Reimer

Report No. 312
November 2000
The Hamburg Ocean-Atmosphere Parameters and Fluxes from Satellite Data (HOAPS): A Climatological Atlas of Satellite-Derived Air-Sea-Interaction Parameters over the Oceans
Hartmut Graßl, Volker Jost, Ramesh Kumar, Jörg Schulz, Peter Bauer, Peter Schlüssel

Report No. 313
December 2000
Secular trends in daily precipitation characteristics: greenhouse gas simulation with a coupled AOGCM
Vladimir Semenov, Lennart Bengtsson

Report No. 314
December 2000
Estimation of the error due to operator splitting for micro-physical-multiphase chemical systems in meso-scale air quality models
Frank Müller
* Atmospheric Environment, 2000 (submitted)

Report No. 315
January 2001
Sensitivity of global climate to the detrimental impact of smoke on rain clouds (only available as pdf-file on the web)
Hans-F. Graf, Daniel Rosenfeld, Frank J. Nober

Report No. 316
March 2001
Lake Parameterization for Climate Models
Ben-Jei Tsuang, Chia-Ying Tu, Klaus Arpe

Report No. 318
March 2001
On North Pacific Climate Variability
Mojib Latif
* Journal of Climate, 2001 (submitted)

MPI-Report-Reference: *Reprinted in

Report 1 - 302 Please order the reference list from MPI for Meteorology, Hamburg

Report No. 319
March 2001
The Madden-Julian Oscillation in the ECHAM4 / OPYC3 CGCM
Stefan Liess, Lennart Bengtsson, Klaus Arpe
* Climate Dynamics, 2001 (submitted)

Report No. 320
May 2001
Simulated Warm Polar Currents during the Middle Permian
A. M. E. Winguth, C. Heinze, J. E. Kutzbach, E. Maier-Reimer, U. Mikolajewicz, D. Rowley, A. Rees, A. M. Ziegler
* Paleoceanography, 2001 (submitted)

Report No. 321
June 2001
Impact of the Vertical Resolution on the Transport of Passive Tracers in the ECHAM4 Model
Christine Land, Johann Feichter, Robert Sausen
* Tellus, 2001 (submitted)

Report No. 322
August 2001
Summer Session 2000
Beyond Kyoto: Achieving Sustainable Development
Edited by Hartmut Graßl and Jacques Léonardi

Report No. 323
July 2001
An atlas of surface fluxes based on the ECMWF Re-Analysis- a climatological dataset to force global ocean general circulation models
Frank Röske

Report No. 324
August 2001
Long-range transport and multimedia partitioning of semivolatile organic compounds:
A case study on two modern agrochemicals
Gerhard Lammel, Johann Feichter, Adrian Leip
* Journal of Geophysical Research-Atmospheres, 2001 (submitted)

Report No. 325
August 2001
A High Resolution AGCM Study of the El Niño Impact on the North Atlantic / European Sector
Ute Merkel, Mojib Latif
* Geophysical Research Letters, 2001 (submitted)

Report No. 326
August 2001
On dipole-like varibility in the tropical Indian Ocean
Astrid Baquero-Bernal, Mojib Latif
* Journal of Climate, 2001 (submitted)

Report No. 327
August 2001
Global ocean warming tied to anthropogenic forcing
Berhard K. Reichert, Reiner Schnur, Lennart Bengtsson
* Geophysical Research Letters, 2001 (submitted)

Report No. 328
August 2001
Natural Climate Variability as Indicated by Glaciers and Implications for Climate Change: A Modeling Study
Bernhard K. Reichert, Lennart Bengtsson, Johannes Oerlemans
* Journal of Climate, 2001 (submitted)

Report No. 329
August 2001
Vegetation Feedback on Sahelian Rainfall Variability in a Coupled Climate Land-Vegetation Model
K.-G. Schnitzler, W. Knorr, M. Latif, J.Bader, N.Zeng
Geophysical Research Letters, 2001 (submitted)

Report No. 330
August 2001
Structural Changes of Climate Variability **(only available as pdf-file on the web)**
H.-F.Graf, J. M. Castanheira
Journal of Geophysical Research -Atmospheres, 2001 (submitted)

Report No. 331
August 2001
North Pacific - North Atlantic relationships under stratospheric control? (only available as pdf-file on the web)
H.-F.Graf, J. M. Castanheira
Journal of Geophysical Research -Atmospheres, 2001 (submitted)

Report No. 332
September 2001
Using a Physical Reference Frame to study Global Circulation Variability (only available as pdf-file on the web)
H.-F.Graf, J. M. Castanheira, C.C. DaCamara, A.Rocha

MPI-Report-Reference: *Reprinted in

Report 1 - 302 Please order the reference list from MPI for Meteorology, Hamburg

Journal of Atmospheric Sciences, 2001 (in press)

Report No. 333
November 2001
Stratospheric Response to Global Warming in the Northern Hemisphere Winter
Zeng-Zhen Hu

Report No. 334
October 2001
On the Role of European and Non-European Emission Sources for the Budgets of Trace Compounds over Europe
Martin G. Schultz, Johann Feichter, Stefan Bauer, Andreas Volz-Thomas

Report No. 335
November 2001
Slowly Degradable Organics in the Atmospheric Environment and Air-Sea Exchange
Gerhard Lammel

Report No. 336
January 2002
An Improved Land Surface Parameter Dataset for Global and Regional Climate Models
Stefan Hagemann

Report No. 337
May 2002
Lidar intercomparisons on algorithm and system level in the frame of EARLINET
Volker Matthias, J. Bösenberg, H. Linné, V. Matthias, C. Böckmann, M. Wiegner, G. Pappalardo, A. Amodeo, V. Amiridis, D. Balis, C. Zerefos, A. Ansmann, I. Mattis, U. Wandinger, A. Boselli, X. Wang, A. Chaykovski, V. Shcherbakov, G. Chourdakis, A. Papayannis, A. Comeron, F. Rocadenbosch, A. Delaval, J. Pelon, L. Sauvage, F. DeTomasi, R. M. Perrone, R. Eixmann, J. Schneider, M. Frioud, R. Matthey, A. Hagard, R. Persson, M. Iarlori, V. Rizi, L. Konguem, S. Kreipl, G. Larchevêque, V. Simeonov, J. A. Rodriguez, D. P. Resendes, R. Schumacher

Report No. 338
June 2002
Intercomparison of water and energy budgets simulated by regional climate models applied over Europe
Stefan Hagemann, Bennert Machenhauer, Ole Bøssing Christensen, Michel Déqué, Daniela Jacob, Richard Jones, Pier Luigi Vidale

Report No. 339
September 2002
Modelling the wintertime response to upper tropospheric and lower stratospheric ozone anomalies over the North Atlantic and Europe
Ingo Kirchner, Dieter Peters

Report No. 340
November 2002
On the determination of atmospheric water vapour from GPS measurements
Stefan Hagemann, Lennart Bengtsson, Gerd Gendt

Report No. 341
November 2002
The impact of international climate policy on Indonesia
Armi Susandi, Richard S.J. Tol

Report No. 342
December 2002
Indonesian smoke aerosols from peat fires and the contribution from volcanic sulfur emissions (only available as pdf-file on the web)
Bärbel Langmann, Hans F. Graf

Report No. 343
January 2003
Modes of the wintertime Arctic temperature variability
Vladimir A. Semenov, Lennart Bengtsson

Report No. 344
February 2003
Indicators for persistence and long-range transport potential as derived from multicompartment chemistry-transport modelling
Adrian Leip, Gerhard Lammel

Report No. 345
February 2003
The early century warming in the Arctic – A possible mechanism
Lennart Bengtsson, Vladimir A. Semenov, Ola Johannessen

Report No. 346
May 2003
Variability of Indonesian Rainfall and the Influence of ENSO and Resolution in ECHAM4 Simulations and in the Reanalyses
Edvin Aldrian, Lydia Dümenil Gates, F. Heru Widodo

MPI-Report-Reference: *Reprinted in

Report 1 - 302 Please order the reference list from MPI for Meteorology, Hamburg

Report No. 347
June 2003

Sensitivity of Large Scale Atmospheric Analyses to Humidity Observations and its Impact on the Global Water Cycle and Tropical and Extra-Tropical Weather Systems
L. Bengtsson, K. I. Hodges, S. Hagemann

Report No. 348
September 2003

EARLINET: A European Aerosol Research Lidar Network to Establish an Aerosol Climatology
J. Bösenberg, V. Matthias, et al.

Report No. 349
November 2003

The atmospheric general circulation model ECHAM 5. PART I: Model description
E. Roeckner, G. Bäuml, L. Bonaventura, R. Brokopf, M. Esch, M. Giorgetta, S. Hagemann, I. Kirchner, L. Kornblueh, E. Manzini, A. Rhodin, U. Schlese, U. Schulzweida, A. Tompkins

ISSN 0937 - 1060